Synthesizing a Heparin Mimic Material Derived from Cellulose Nanocrystals

Zahra Jane Gallagher

Thesis submitted to the faculty of the Virginia Polytechnic Institute and State University in partial fulfillment of the requirements for the degree of

Master of Science
In
Materials Science and Engineering

E. Johan Foster
Neil Ayres
Aaron Goldstein

June 28, 2018
Blacksburg, VA

Keywords: Nanocrystalline cellulose, heparin mimic, anticoagulation, hemodialysis

Synthesizing a Heparin Mimic Material Derived from Cellulose Nanocrystals

Zahra J. Gallagher

Abstract

To prevent clotting during dialysis, heparin is used to line the tubing which blood flows through. Unfortunately, many side effects arise from taking heparin, especially when it is used for an extended period of time. As such, long-term exposure for individuals undergoing dialysis every day is unavoidable. To prevent the solubilized heparin from entering the bloodstream, a polymer-based natural material is being investigated. This materials properties include reduction of coagulation and elimination of the long-term effects of heparin such as heparin induced thrombocytopenia and osteoporosis.

Cellulose nanocrystals (CNCs) contain the same 1,4 linked pyranose backbone structure as heparin along with desirable mechanical properties, like high stiffness and anisotropic shape. By altering the functionalization on the surface of CNCs to closely mirror that of heparin, it should be possible to make a biomimetic material that counteracts blood clotting, while not introducing soluble small molecule anticoagulants into the body. Through blood assays and platelet fixing analysis, we have been able to show that this change in functionalization does reduce coagulation. Surface chemistry of CNCs were modified from 'plain' CNCs (70 mmol SO_3^-/kg residual from hydrolysis) to 500 mmol COO^-/kg (TEMPO oxidized) and 330 mmol SO_3^- /kg CNC (sulfated CNCs). We will show that by utilizing CNCs reactive functional groups and incredible mechanical properties we are able to create a material that reduces clotting while maintaining the tubing's mechanical strength as well as eliminating heparin's side effects associated with it being a soluble anti-coagulant.

Synthesizing a Heparin Mimic Material Derived from Cellulose Nanocrystals

Zahra J. Gallagher

General Audience Abstract

To prevent clotting during dialysis, heparin is used to line the tubing which blood flows through. Heparin, an anticoagulant, is more commonly known as a 'blood thinner' which is a misnomer because it does not actually thin blood. Heparin works by inhibiting clotting factors in the coagulation cascade pathway which in turn limit the formation of blood clots and create the 'thinning' effect mentioned earlier. When dialysis is performed the interaction between blood and the dialyzer tubing initiates the formation of a blood clot. This is where heparin use comes in. Unfortunately, many side effects arise from taking heparin, especially when it is used for an extended period of time. As such, long-term exposure for individuals undergoing dialysis every day is unavoidable. To prevent heparin or its mimics from entering the bloodstream, a polymer-based natural material is being investigated. The properties of this material will include reduction of coagulation and elimination of the long-term effects of heparin.

The polymer-based natural material being investigated is cellulose nanocrystals (CNCs). CNCs contain the same ring structure and chemical linkage sites as heparin along with desirable mechanical properties. By altering the surface chemistry on the CNCs to closely mirror that of heparin, it should be possible to make a biomimetic material that counteracts blood clotting, while not introducing a solution based small molecule anticoagulant to the body. Through blood assays and platelet fixing analysis, we have been able to show that this change in functionalization does reduce coagulation. The 'plain' CNCs used contained an initial charge density of 70 mmol SO_3^-/kg. This residual charge density was a result from the acid hydrolysis performed to acquire CNCs from cellulose. Chemically modified CNCs contained many more negatively charged functional groups with TEMPO oxidized and sulfated CNCs having 500 mmol COO^-/kg and 330 mmol SO_3^-/kg, respectively.

We will show that by utilizing CNCs reactive functional groups and incredible mechanical properties we are able to create a material that reduces clotting while maintaining the tubing's mechanical strength as well as eliminating heparin's side effects associated with it being a soluble anti-coagulant.

Acknowledgements

I must express my profound gratitude to my advisor, Dr. E. Johan Foster, for bringing me into his lab during my undergraduate degree and allowing me to continue research through my graduate. I will forever be grateful for the opportunities you have given me the past three years. From Switzerland to my Master's degree, none of this would have been possible without your help and support. Thank you to my research group, especially Chris Rader, for helping brainstorm and letting me talk through different, sometimes impractical, ideas. Thank you to the members of my committee, Dr. Neil Ayres and Dr. Aaron Goldstein, for your hard work and observations. Lastly, I would like to thank my parents for their encouragement, for believing in me, and helping me throughout this process.

Table of Contents

List of Figures and Tables In Introduction

Purpose

Current anticoagulation treatment for end-stage renal disease (ESRD) patients during hemodialysis (HD) includes intravenous administration and/or lining dialysis tubing with heparin. An estimated 1.5 million people in the world undergo dialysis treatment with about 90% using hemodialysis.[8] These patients' kidneys function at 15% or less of an average individual's kidney function. With half of heparin metabolized in the kidneys, lower function creates a build up of heparin in the body. HD patients often undergo the procedure three times a week for four hours with heparin being administered several times during the procedure. This constant heparin use can cause several negative side effects including hemorrhage, heparin induced thrombocytopenia (HIT), hypersensitivity, elevations of aminotransferase, and osteoporosis. Patients with HIT are at high risk for venous or arterial thrombosis and the osteoporosis that is caused by heparin is irreversible. Unfractionated heparin (UFH) and low-molecular-weight heparin (LMWH) can cause HIT, with UFH patients at an increased risk. Ultra-low-molecular-weight heparin (ULMWH) does not cause HIT, showing this form of heparin relies on the molecular weight of the sample. Osteoporosis caused by heparin hinders the differentiation and function of osteoblasts while also increasing the number of osteoclasts resulting in a loss of bone density.[9] The change in bone density is unable to be mitigated after the patient stops taking heparin.

Medical grade heparin is manufactured through animal by-products, often porcine or bovine intestine. This creates a situation in which heparin is at a high risk of contamination. When bovine spongiform encephalopathy, or mad cow disease, infected cows in 2014, concerns arose about a risk of the prion entering the heparin supply. This event generated a recall of all heparin manufactured from bovines. A similar event has the potential to reoccur, potentially leading to a recall of UFH and LMWH. It is possible that the world supply of heparin could be suspect if such an outbreak occurred. By converting some of the heparin supply from animal based to synthetic based, the negative effects of an outbreak on heparin supplies could be greatly mitigated.

Current materials used during HD do not actively inhibit clots from forming. This is why patients need heparin administration during their HD treatments. The different material characteristics of HD tubing stimulate clots to form, forcing patients to take heparin or anticoagulant free HD which is much more complicated. To reduce or eliminate the need for heparin therapy a material would either need to have the characteristics similar to a blood vessel

and/or inhibit the coagulation cascade. Factors that limit coagulation are surface free energy and wettability, surface chemistry and functional groups, and topography and roughness.[6] Hydrophilic surfaces, negatively charged functional groups, and topography mimicking that of blood vessels has the potential to create the ideal *ex vivo* material environment for blood flow.

The functionalization and purity of the heparin mimic will also be able to be better controlled through synthesis. This production method also eliminates the risk of animal derived contamination and the negative side effects that come with it. This is because the side effects caused by heparin are only induced by solubilized heparin *in vivo* that interact with elements in the system. CNCs create suspensions, not solutions, and so when added to a CNC material made to mimic heparin the material will not release any compounds into the blood stream, removing any unintentional compound interaction. Creating a CNC material that mimics heparin will reduce the cost, side effects, and dependability on an animal derived product. Focusing on HD, if a material with the properties proposed is produced then the 1.35 million HD patients would not have to worry about how their treatment could affect their health.

1 Introduction

1.1 Heparin

1.1.1 Background

Anticoagulants are chemically synthesized, naturally occurring, or semi-natural substances that reduce coagulation through the suppression of clotting factors. Coagulation, i.e. blood transforming from a liquid to a gel, results when the endothelium lining of a blood vessel is damaged or external trauma affects the vascular system. This damage and repair process, called hemostasis, is regulated by anticoagulant and procoagulant concentrations kept balanced to maintain equilibrium. The reduction of coagulation can reduce, treat, or prevent the risk of blood clots breaking off and traveling through the bloodstream to organs and prevent blood from clotting during surgeries or dialysis treatment. Diverse anticoagulant compounds reduce coagulation by distinct methods, but most inhibit the coagulation cascade. A wide range of blood-related operations and devices can be accomplished now by using anticoagulants. Medical treatments that utilize anticoagulants range from thrombosis, embolisms, kidney dialysis, cardiopulmonary bypass, and the prevention of clotting in surgery.[10-11]

One of the most widely used and efficient anticoagulants is heparin, with thirty percent of hospital patients being exposed to it in the United States.[12-14] Heparin is a linear, sulfated, and negatively charged polysaccharide biosynthesized in the Golgi of mast cells within the glycosaminoglycan (GAG) class.[9, 15-18] The basic structure of heparin is composed of α-1,4 linked uronic acid and D-glucosamine. The principal use of heparins has been for anticoagulation, but its interactions with more than 400 proteins are starting to be investigated.[19] These interactions include, but are not limited to, binding and inhibiting cellular adhesion molecules[20-21], enhancing stimulation of fibroblast growth factor receptor signal transduction[22-23], binding to inflammatory cytokines[24-25], and stimulating anti-inflammatory activity through the reduction of LPS-induced nuclear translocation of NF-κβ [20-21].

The average molecular weight of pharmaceutical grade heparin is 15,000-19,000 Da with a polydispersity index of 1.1-1.6.[11, 26-27] To restrict coagulation, a heparin chain, with a minimum length of 18 residues, interacts with the serpin plasma cofactor antithrombin III (AT).[12, 15, 28-30] This interaction causes a conformational change in AT that inhibits the clotting factors Xa and thrombin (IIa).

The anti-thrombin binding region (ATBR) is a pentasaccharide sequence within AT that heparin binds to in order to initiate the inhibition of the clotting pathway.[13, 26] Roughly 1% of vessel-wall heparin and one-third of mast cell heparin contains the ATBR.[26, 28, 30-31] This binding sequence, shown in Figure 1, is composed of GlcNAc6SO_3 - GlcA-GlcNSO_3-3-6SO_3 - IdoA2SO_3 - GlcN$SO_3$6SO_3. Of these groups, the most important to AT binding is GlcNSO_3-3-6SO_3.[15]

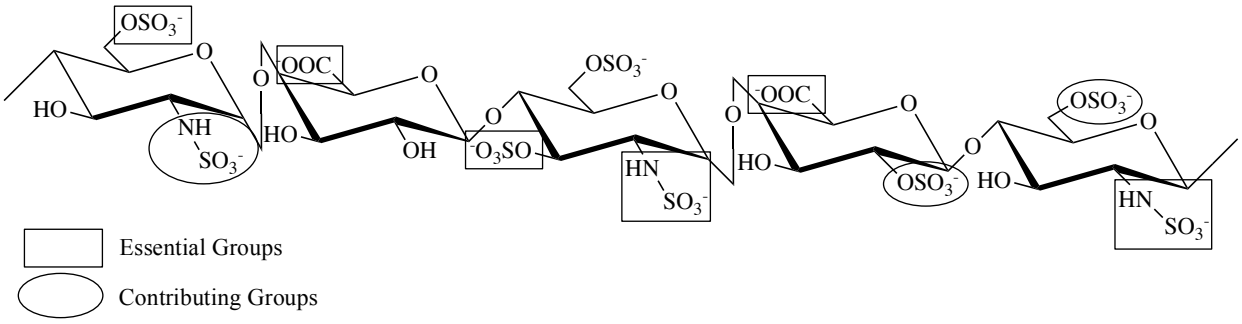

Figure 1: Antithrombin binding region within heparin

The anticoagulant properties of heparin are due to its high negative charge. Compared to other naturally derived biomolecules, heparin has the highest negative charge density with a total charge of approximately 75 mmol negative charge density/kg.[9] The main functional groups that provide this charge are the carboxyl, O-sulfation, and N-sulfation groups. These groups interact with biomolecules through electrostatic interactions derived from positively charged amino acids in the target proteins binding site.[9, 26, 32] Electrostatic interactions are characterized as any non-covalent bonds, which all biological structures and processes rely on. The sulfur content of heparin, which contains most of the negative charge density, corresponds to about 2.5-2.7 sulfate groups per disaccharide unit.[9, 16, 29]

Current heparins used are unfractionated heparin (UFH), low molecular weight heparin (LMWH), and ultra-low molecular weight heparin (ULMWH). Each activates the cascade pathway uniquely and is administered differently. UFH is taken intravenously while LMWH and ULMWH are taken subcutaneously. Drugs taken intravenously are administered directly into the blood stream making them immediately available, but also immediately metabolized. When administered subcutaneously, the lack of blood vessels in the area results in a slow release into the system. Heparin can be administered subcutaneously but the activity is initiated after 20-60 minutes.[33] Often, when anticoagulation of the blood is needed immediately UFH will be administered,. LMWH and ULMWH are taken subcutaneously and have near 100%

bioavailability. This is partially because of the subcutaneous administration method and the fact that larger chains, like UFH, are cleared from the system faster.[34-36] Subcutaneous delivery benefits patients by producing less discomfort at the injection site as well as generating a longer onset of activation, which then creates a longer half-life.

1.1.2 Biochemistry

The numerous pathways used for various complexes can be ascertained by different anticoagulant tests.[9] Heparin interacts through secondary hemostasis, commonly known as the coagulation pathway, shown in Figure 2, through two methods. The first is by creating a tertiary complex between AT, heparin, and thrombin (shown in figure 3). This complex is able to be formed when a complex is 18 residues long, shorter chains utilize a binary complex method. This binary method forms when the ATBR in heparin interacts with AT to undergo a conformational change which creates a heparin/AT complex.[37-38] This complex allosterically activates the pathway and exposes arginine residues on AT which covalently bind to specific serine residues on serine proteases to inhibit their function.[11] Serine proteases, also known as coagulant enzymes, that can be inhibited are factors IX, X, XI, XII, and prothrombin (factor II).[18, 39] Thrombin (IIa) and factor Xa are the most sensitive to inhibition, with thrombin being 10-fold more sensitive, and effect coagulation the greatest so these will be focused on.[15]

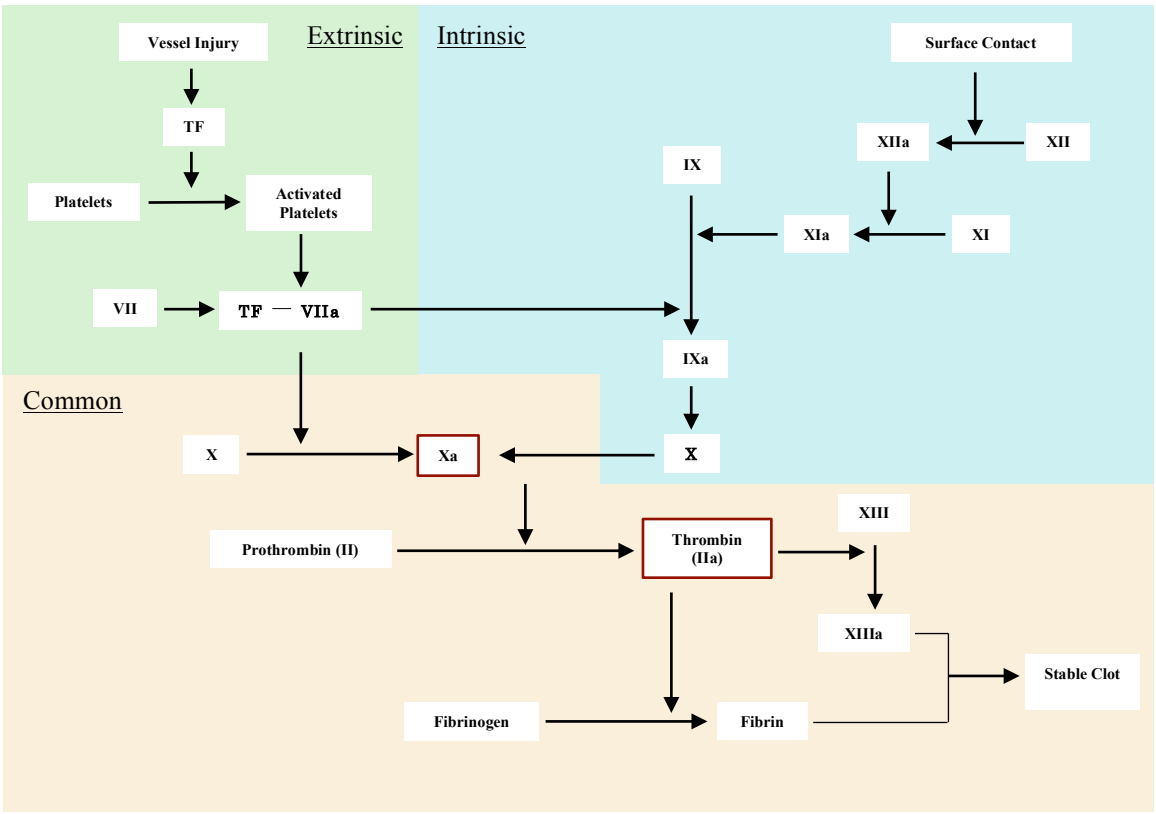

Figure 2: Coagulation cascade pathway, with the factors most affected by heparin and its derivatives, factors Xa and IIa (thrombin), outlined in red[5]

To form the bridging ternary complex, heparin chains must be greater than 18 residues long.[40] Without bridging, thrombin inhibition is unable to be catalyzed and only factor Xa is inhibited through the binary complex. Fibrin formation (the process that forms clots along with platelets) and inhibition of thrombin-induced activation of factor V and VIII will take place if thrombin is inhibited.[41]

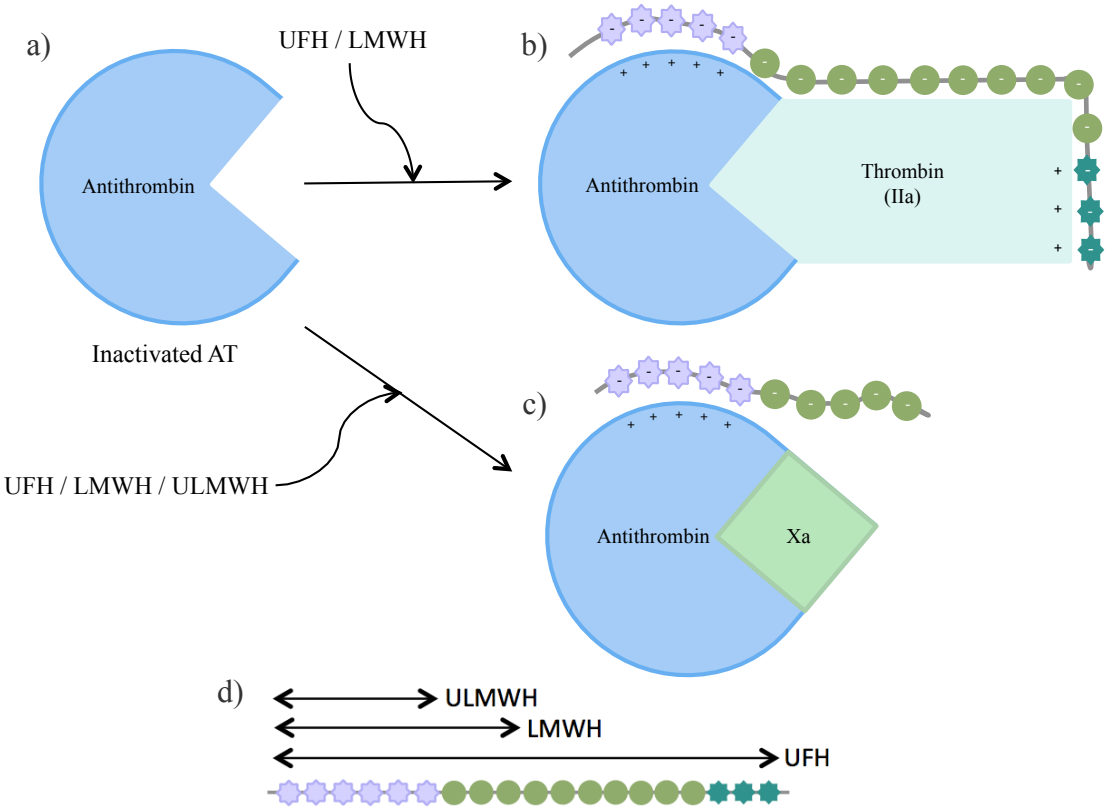

Figure 3: a) Inactivated antithrombin b) Activated AT-thrombin complex formed by an 18 residue or longer heparin chain c) Activated AT-Xa complex formed by a heparin chain with functional groups similar to the ATBR d) Chain length of ultra-low-molecular-weight heparin, low-molecular-weight heparin, and unfractionated heparin compared to the heparin chain imaged in b and c

Even without bridging, as long as there is the ATBR that binds to AT, heparin is still able to reduce coagulation.[39] The loss of the bridging mechanism is utilized in 50-75% of LMWH and all of ULMWH.[27] We are focusing on the loss of bridging and heparin-Xa binding in our anticoagulant material because it will not be in the system and thus be able to 'wrap' around to form a ternary complex. Figure 3 shows how chain length can affect the bridging process. Loss of bridging also changes the ratio of anti-IIa and anti-Xa activity because with no bridging there is no anti-IIa activity. LMWH's ratio of anti-IIa to anti-Xa activity vary from 3.9:1 to 1.6:1 depending on the depolymerization, while in UFH the ratio is about 1:1.[39-40] This lowered binding affinity to create the AT/thrombin complex has a benefit; with lower thrombin activity comes a lower risk of hemorrhaging.[42] The different levels of this ratio for different heparin derivate is shown in Table 1.

Table 1: Comparison of commonly used anticoagulants

Type	Brand	Avg Molecular Weight (Da)	Half-Life (hours)	Ratio Anti Xa/Anti-thrombin Activity	Administration	Price per Dose (USD)	Approved Market	References
Unfractionated Heparin	---	15,000-19,000	1.5	1	Intravenous	1-2	Worldwide	43, 44, 45
Low-Molecular-Weight Heparin	Enoxaparin (Lovenox)	4,500	4.5-7	3.9	Subcutaneous	3-13	USA, Germany, Spain	44, 46, 47
	Dalteparin (Fragmin)	6,000	2-5	2.5	Subcutaneous	152-157	USA, Germany Japan, UK	44, 45, 46
	Tinzaparin (INNOHEP)	6,500	3-4	1.6	Subcutaneous	Unavailable	Germany, Denmark	44, 46, 48
Ultra-Low-Molecular-Weight Heparin	Fondaparinux (Arixtra)	1,700	17-21	0	Subcutaneous	3,000-7,000	USA	43, 44, 46, 49
Vitamin K Antagonists	Warfarin (Coumadin)	308	36-42	n/a	Orally	0.15-0.5	Worldwide	50

Heparin is cleared from the system by two methods, a primary and a secondary. The primary method involves heparin binding to receptors on membranes of endothelial cells and macrophages.[41] The heparin is recognized by cell surface receptors, which stimulate the cell to internalize then depolymerize the heparin. Longer chains have a higher affinity to the cell surface receptors. The second method involves heparin eliminated through renal clearance. This is a much slower process, so the half-life of heparin depends on the dose. At a small dosage, only the primary method is used, giving it a low half-life. At a high dosage, the primary method is saturated making both methods used, therefore producing a longer half-life.[39]

1.1.3 Isolation

Heparin can be found in the mast cells of a wide range of animal's intestines, lungs, liver, and skin.[46] Suitable animals range from turkeys to zebra fish. The first heparin sources were derived from canine and bovine livers. Later, canine livers were phased out, and porcine mucosa was introduced. Currently, heparin is isolated and extracted from porcine intestine, bovine lung, bovine intestine, and ovine intestine. [16, 26, 43] In the US the only FDA approved

source of heparin is porcine mucosa because of the risk of contamination with bovine spongiform encephalopathy, which causes mad cow disease.[44] Porcine mucosa has also been found to requires less degradation.[38] Additionally, bovine and ovine heparin have approximately half the enzymatic activity compared to porcine heparin.[11, 45]

Each year 24 tons of heparin is administered in the US with the concentration of heparin in its starting material being ~160-260 mg/kg.[26] To meet the annual need of heparin the intestines of ~1 billion pigs (1 pig can produce ~3 doses of UFH or ~1 dose of LMWH) are collected from slaughterhouses.[38, 43] Focusing on porcine mucosa, the process of recovering heparin is performed by removing the matter containing glycosaminoglycan's within the intestines then soaking them in a salt solution. Once soaked, the mucosa is scraped out and hydrolyzed to create primary heparin. This heparin is then added to an anion exchange resin to filter out the hydrolysate. A preservative is added, and the heparin is shipped for primary testing to make sure no prion antigens are present, the heparin is derived from the animal species indicated, and if there is any over-sulfated chondroitin sulfate (OSCS) in the batch. This testing is due to the 2008 heparin contamination mentioned later. After this screening process has been completed and the product is found to meet standards, additional chemical processing is carried out to create purified, pharmaceutical-grade heparin.[46] This processing includes an oxidation step, which removes possible endotoxins, bacteria, mold, viruses and prions from the system.[38] The final heparin product is acquired by taking the chemically processed heparin and diluting it with water then filtering it through a 1000 molecular weight membrane and a 0.22 micron membrane, and then lyophilizing it. This is a broad overview on the procedure; the exact techniques, concentrations, and solvents used during the extraction of heparin are tightly guarded industrial secrets.

1.1.4 Heparin Derived Drugs

1.1.4.1 Unfractionated Heparin

The most common and preferred form of heparin is unfractionated heparin (UFH). Before LMWH was produced, UFH was the most common source of heparin, but it now accounts for only approximately 4% of the the anticoagulation market.[11] Each year 100 tons of UFH is produced around the world.[43] The use of heparin is less than that of other anticoagulants due highly to its heterogeneous nature from it being assembled in a non-template directed method in the body. The non-uniform structure results in heterogeneous interaction with proteins

and AT.[38] Studies show, that a variable heparin dose is required for different patients making outpatient treatment more difficult.[47]

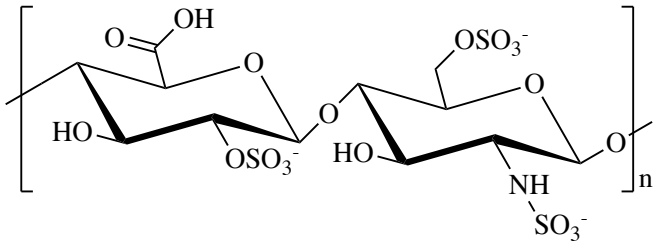

Figure 4: Basic structure of unfractionated heparin

Removal of UFH from the body utilizes both the primary and secondary method. Those with kidney failure are advised to use UFH over other forms of heparin so heparin does not accumulate in their kidneys (1.1.4.3 Low-Molecular-Weight Heparin).

Reversal of UFH can be done by adding protamine sulfate (PS) into the system intravenously.[35] PS is a strongly basic, highly cationic, peptide derived from fish sperm that reduces heparin's activity through direct binding interaction.[48] The amino acid sequence of PS is ARYRC CRSQS RSRYY RQRQR SRRRR RRSCQ TRRRA MRCCR PRYRP RCRRH.[49] Arginine, a positively charged amino acid, makes up the majority of PS' amino acid composition.[50] PS dissociates the heparin-AT complex and the guanidino group within arginine interacts with heparin to create a complex through electrostatic interactions and ion pairing.[51-52] This lowers the bioavailability of heparin to bind to AT and creates a stable salt.[53] Protamine has a half-life of seven minutes with the ability to dissociate heparin from AT within five minutes, eliminating the anticoagulant effect .[54]

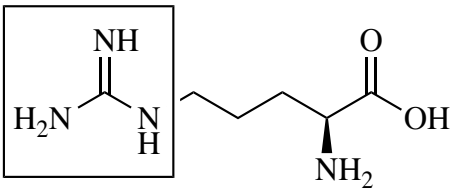

Figure 5: Arginine amino acid with the guanidino group in a square

1.1.4.2 Heparin Sulfate

Heparin sulfate (HS) is a GAG that is biosynthesized from heparin sulfate proteoglycans (HSPGs), which are expressed and secreted by almost all mammalian cells.[55] HS contains the same backbone structure as heparin, but the components within it are proportionally different. Compared to heparin, HS has a much higher average molecular weight, larger polydispersity index, and distribution of undersulfated domain as seen in Figure 6. *In vitro* the functions of HS

are linked to HSPGs. These functions include but are not limited to anticoagulation, playing a key role in angiogenesis, cell adhesion, regulation of cellular growth and proliferation, inhibition of blood coagulation, and cell surface binding of lipoprotein lipase and other proteins.[55] HSPGs have a half-life of 2-24 hours with complete elimination from the body in 48 hours.[56] With a degree of sulfation value of 0.5-1.5 sulfate groups per disaccharide, HS is unable to limit coagulation effectively compared to heparin.[7] Only about 1-10% of HS isolated from tissues are able to bind to AT.[57] This low yield and anticoagulation efficiency limits HS from entering the anticoagulant market and being a viable alternative to heparin.

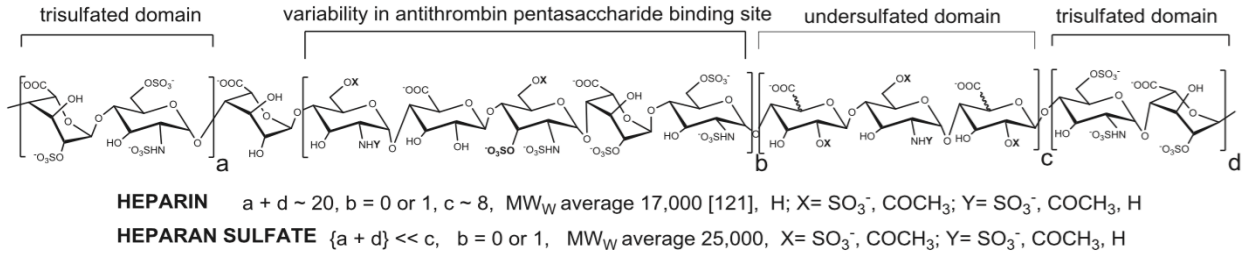

Figure 6: Difference in structure of heparin and heparin sulfate[7]

1.1.4.3 Low-Molecular-Weight Heparin

Low-Molecular-Weight Heparin (LMWH), also sometimes called fractionated heparin, include enoxaparin, finixaparin, tinzaparin, and five other clinically approved LMWH, makeup 50% of the heparin market.[11, 58] LMWH is composed of 16-20 monosaccharide units per heparin with and is derived by chemical or enzymatic controlled depolymerization from UFH.[59] Compared to UFH, LMWH has better bioavailability, a longer half-life, and dose-dependent clearance.[27, 40, 60]

The different types of LMWH are created by different depolymerization reactions of UFH. Since the ATBR is only present in one-third of heparin, LMWH is formulated to be one-third the weight of heparin giving it a molecular weight range of 3,500-6,000 Da with an average of 4,500 Da.[35, 58] By reducing the length of UFH and concentrating the ATBR, LMWH has greater, more specific binding to factor Xa than to thrombin as well as reduced binding to plasma proteins and endothelium. Due to the primary clearance pathway having a higher affinity to longer heparin chains, the secondary clearance pathway mainly dictates the removal of LMWH from the body. The lower binding along with using mainly the secondary clearance method increases the half-life from UFHs 1.5 hours to 4.5-7 hours.[39-40] The LMWH of choice is enoxaparin, with a half-life of 4.5 hours.[58] The doses do not need monitoring or adjustments

because binding is predictable and the risk of bleeding does not increase, so it is a safe at home alternative.

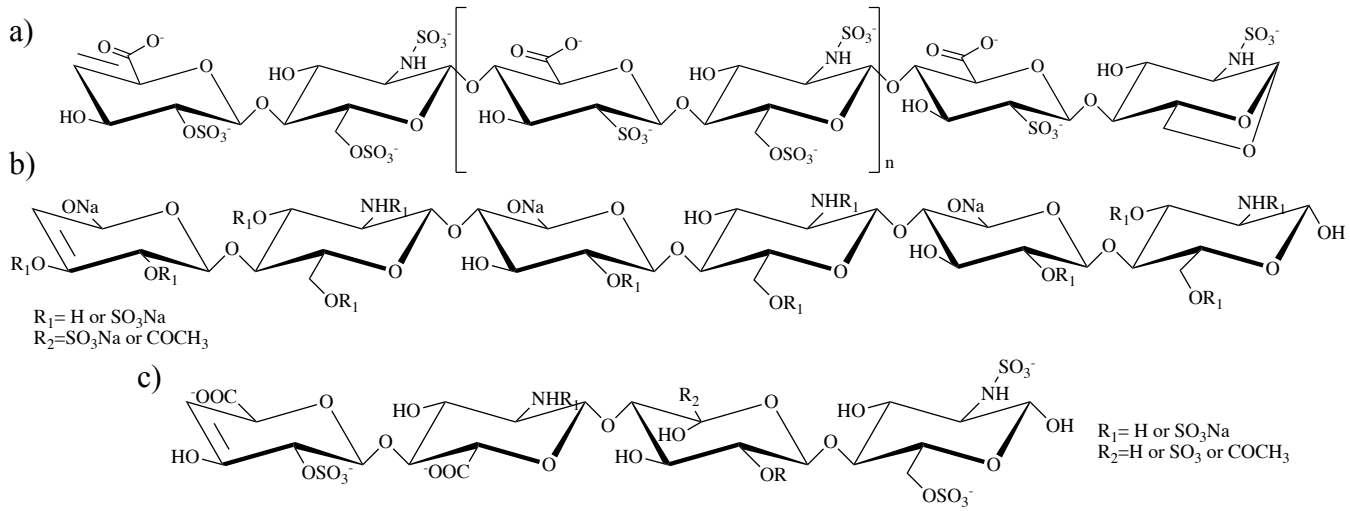

Figure 7: Structure of several common low-molecular-weight heparins a) Enoxaparin b) Bemiparin c) Tinzaparin

The binding of LMWH is predictable because it is depolymerized to create a more homogeneous structure with less nonspecific plasma protein binding than that of UFH. This predictability as well as its ability to be subcutaneously administered allows LMWH to be used in an outpatient setting. Similar to UFH, in case of an overdose the antidote, protamine, can be administered. It should be stated that not all LMWH's react with protamine to stop anticoagulation. Unlike UFH, only factor Xa activity can be reversed when using protamine on LMWH.[61] The main reason behind LMWH not being fully neutralized is due to reduced sulfation.[62] LMWH's that have higher sulfonation can be neutralized more than those with lower sulfation.

LMWH has reduced binding to platelet factor 4 (PF4) and osteoclasts. The reduced binding to osteoclasts decreases the incidence of osteoporosis (1.1.8 Drawbacks of using Heparin).[27] The use of LMWH with patients with kidney impairment is not recommended because reduced binding with cellular receptors for clearance from the body increases releasing heparin through the kidneys. Instead, UFH is recommended because of its higher binding with cellular receptors.[27, 60]

1.1.4.4 Ultra-Low-Molecular-Weight Heparin

Ultra-low-molecular-weight heparins are heparin derivatives or mimics having an average molecular weight of less than 3,000 Da. Examples of this are AVE5026, RO-14, and fondaparinux sodium (Arixtra). AVE5026 and RO-14 are synthesized by selective chemical depolymerization through β-elimination from UFH. Synthesis of AVE5026 is a six-step process.[35] Fondaparinux is chemically synthesized by block synthesis that yields about 0.1% and takes about 55 steps.[63] The result is a pentasaccharide sequence that mimics the ATBR other than a residue on the reducing end. Although AVE5026 and RO-14 are promising ULMWH's, only fondaparinux has been approved after going through thorough testing and is available in the market.

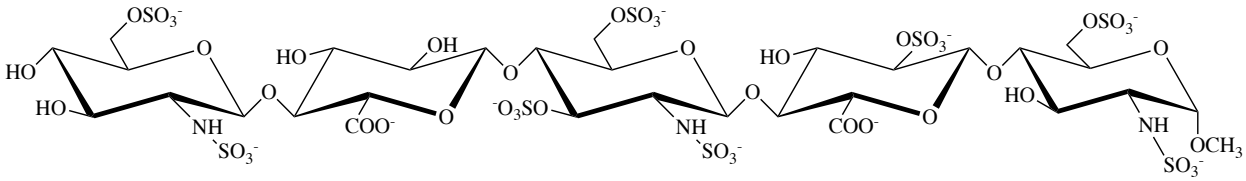

Figure 8: Fondaparinux Sodium (Arixtra)

Due to its extremely low molecular weight, ULMWH inhibits factor Xa with little interaction with thrombin. This inhibition also contributes to ULMWH to having the lowest rate of bleeding, compared to LMWH and UFH.[42] The binding of ULMWH is specific to AT, so unlike UFH, it will not bind to other proteins. The amount administered is used principally in anticoagulation. Weight or age do not affect ULMWH's dose rate, and the pharmacological effects are predictable, so they can be administered at home with no risk.

ULMWH is cleared primarily in the kidneys and can build up, so those with renal impairment are advised not to take it.[35] It should also be warned that those without renal impairment still have the potential for ULMWH to build up in the kidneys. Concentrations in the body can be monitored using the half-life. Fondaparinux has a half-life of 17-21 hours, which is much greater than that of LMWH and UFH as seen in table 1. [42, 64]

ULMWH seems to be a viable option within the heparin product market, though it does have some drawbacks such as low yield and high cost. These characteristics have kept ULMWH comsumption below that of LMWH and UFH. The synthesis of FDA-approved ULMWH has many complex steps, with little yield, which makes it difficult to synthesize at low costs. However, ULMWH offers an alternative that comes without a contamination risk that characterizes animal-derived heparin UFH and LMWH. Should animal-derived heparin be

affected by an outbreak among animal hosts and removed from the market, ULMWH would remain available because of its synthetic origins, creating a potentially indispensible product. This benefit though is limited because the production of ULMWH cannot be relied upon to mitigate a crisis if today's heparin production were removed. Its high cost and low production could not meet the global need of the projected $16.3 billion heparin market in 2025. The limited value, because its clearance is through the kidneys, of ULMWH for kidney dialysis patients also creates a large gap in patients' anticoagulant needs.[43] Another shortcoming of FDA approved ULMWH is that if hemorrhaging or an overdose occurs there is no antidote to stop the anticoagulation. This poses a threat to patients whether they are administered in a hospital or at home.[36] The creation of various types of heparin mimics through synthesis, like ULMWH, would provide an important alternative to prevailing, existing drugs while lowering the likelihood that a contamination crisis steming from animal impurities could fundamentally upend the viability and availability of treatments available.

1.1.5 Heparin Mimics

Many variations of heparin mimics have been synthesized, ranging from polyureas with sulfated carbohydrates to polyaromatic anionic compounds.[9, 63] These mimics have varying structures, but all contain a organosulfate. The next most abundant functionalization added was a carboxyl group. Several mimics contain the N-sulfation group. But many do not, likely because it is much more difficult and chemically hazardous to synthesize. A review of many different heparin mimics can be seen in *Heparin-Mimicking Polymers- Synthesis and Biological Applications*.[9]

1.1.5.1 Chitosan

Chitosan, a deacetylated analog of chitin, is composed of D-glucosamine and N-acetyl-D-glucosamine residues. Chitin is the most abundant natural polymer in the world after cellulose. It is found in the exoskeleton of crustaceans and insects as well as the cell walls of fungi. Chitosan is a desirable compound because of its biocompatibility, biodegradability, and natural antibacterial properties. Before sulfation, chitosan contains coagulation properties that stimulates platelet formation and erythrocyte aggregation.[65] Yang's study on chitosan shows that, after sulfation, chitosan limits coagulation in blood clotting assays relatively well, but not as well as heparin itself.[66] It shows that the greatest anticoagulation effect the sulfated chitosans have is on the activated partial thromboplastin time (aPTT) assay. The thombin time (TT) assay has an

extended clotting time compared to the control, but is far from the anticoagulation level of heparin. Between heparin and sulfated chitosan the TT assay show no change. Another study by Suwan showed that the anticoagulation effect of sulfated chitosan is dictated by the molecular weight.[67] The lower the molecular weight of the sample, the longer the aPTT anticoagulation activity and shorter the TT anticoagulation activity. These results show that sulfated chitosan anticoagulation can be tuned by molecular weight for either the intrinsic or extrinsic pathway. Sulfated chitosan is a versatile, cheap, and abundant resource that shows potential to be the next widely used heparin mimic.

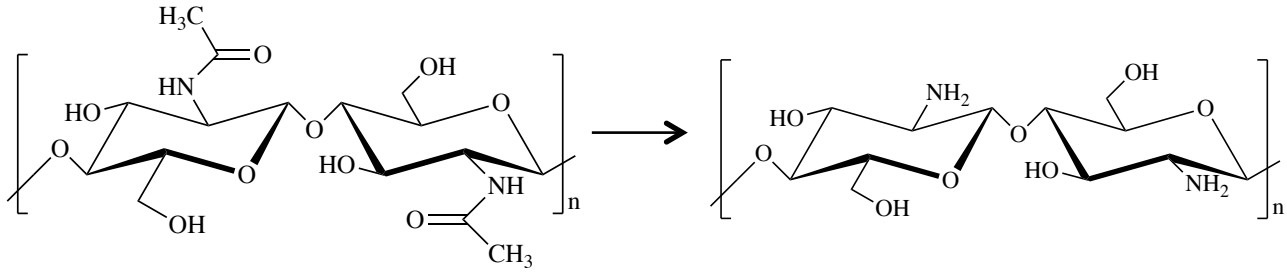

Figure 9: Chitin structure and its deacetylated analog, chitosan

1.1.5.2 Chondroitin Sulfate

Chondroitin sulfate is found on cell surfaces in the extracellular matrix attached to proteins that are part of a proteoglycan. It is a GAG composed of alternating D-glucuronic acid and N-acetyl D-galactosamine residues. Each disaccharide unit contains an average of one sulfate group at the C-4 or C-6 position on the N-acetylated D-galactosamine residude.[68] Similar to heparin, chondroitin sulfate has a very heterogeneous structure. Alone, chondroitin sulfates do not have any appreciable anticoagulation activity because their degree of sulfation is so minimal. To increase their anticoagulation effects Maruyama 'oversulfated' the chondroitin sulfate by adding two to three sulfate groups to each disaccharide.[68] These results proved promising *in vitro* but the 2008 hepatin contamination where heparin was cut with oversulfated chondroitin sulfate proved that it is harmful when administered to humans. The chondroitin sulfate that was used in the contamination contained a tetrasulfated glucuronic acid, similar to Maruyama's work. [69] Section 1.1.8 Drawbacks of Using Heparin talks further about the lethal contamination.

1.1.5.3 Dermatan Sulfate

Dermatan sulfate (DS) is an epimerized chondroitin sulfate where the carboxyl groups are converted from D-glucuronic acid residues into L-iduronic acid resides. This may prove beneficial for creating a heparin mimic, because heparin is composed of iduronic acid residues.

Although the structure of DS is closer to heparin than chondroitin sulfate, the degree of sulfation of DS if still much lower than heparins. This is because its structure consists of mainly N-acetylated residues and nonsulfated uronic acid residues.[70] With fewer sulfate groups on DS, it has fivefold less affinity to AT than heparin. DS still has the ability to bind to AT and create a complex, but only 5% of DS obtained from porcine skin has this binding ability. Other than anticoagulation, DS can bind with other molecules in the body like matrix molecules, growth factors, protease inhibitors, cytokines, chemokines, and pathogen virulence factor.[71]

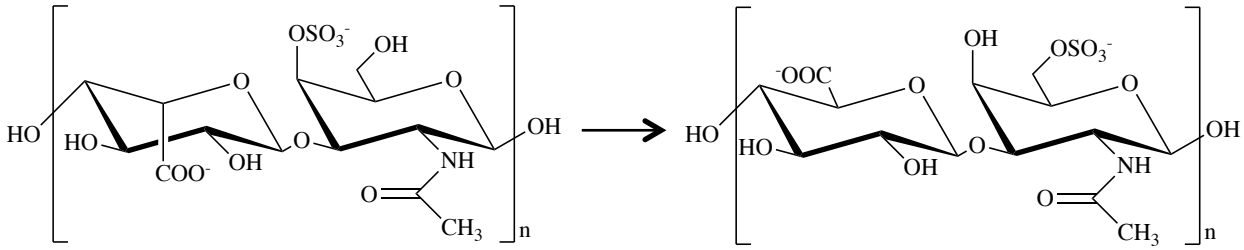

Figure 10: Chondroitin sulfate and its epimerized derivative dermatan sulfate

1.1.5.4 Alginates

Alginate is a linear polysaccharide found in the cell walls of brown seaweed. It is made up of D-mannuronic acid (M) and α-L-gluteronic acid (G) units. Each unit of alginate contains a carboxyl group, which makes it the only natural polysaccharide with this feature.[72] After sulfation of hydroxyl groups, alginate chemically looks similar to heparin with carboxyl and sulfate functional groups along with uronic residues. Ronghua's study on sulfated alginates show that they increase the anticoagulation effects on aPTT assays, but had a minimal effect on TT or PT assays.[72] The aPTT results showed a prolonged anticoagulant effect compared to heparin. These studies show that alginates specifically inhibit the intrinsic pathway of the coagulation cascade, similar to heparin. Along with anticoagulation, alginate has shown to have several other functions such as heparinase inhibition, anti-oxidation, anti-HIV, anti-inflammation, and preventing calcium phosphate crystal formation in the urinary tract.[73]

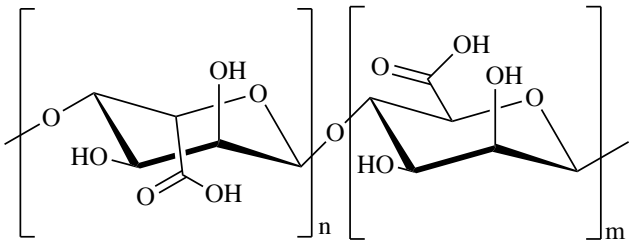

Figure 11: Structure of alginate

1.1.5.5 Sulfated Carbohydrates and Polysaccharides

Sulfated carbohydrates and polysaccharides used as heparin derivatives range from monomer saccharides that are polymerized to naturally occurring polysaccharides, like pullulan and sulfated dextran. The degree of anticoagulation these substances are able to achieve is directed by their degree of the sulfation, molecular weight, and position of sulfate groups. To have the potential ability to induce anticoagulation all saccharide structures must contain clusters of negatively charged sulfate groups.[74] After further investigation and understanding of what stimulates anticoagulation chemically synthesized polysaccharides over naturally derived polysaccharides began being developed.[75]

Several different methods have gone into studying sulfated polysaccharides. Huang looks at chemically altering polyurethane by attaching lactose, mannose, and glucose residues then sulfating the hydroxyl groups on the cabohydrates.[63] This research proved that by altering polyurethanes structure through the addition of sulfated carbohydrates the hemocompatibility can be improved. Another study looks at sulfonating pullulan, an exopolysaccharide that is produced by the black yeast *Aureobasidium pullulans*.[76] This study looks at the effect of degree of sulfation, reaction time and temperature, and location of sulfation on sulfated pullulan's anticoagulation effects. The results are similar to other studies where higher temperatures and longer amounts of time gave a higher degree of sulfation. The location of sulfate groups bound did not seem to have an effect on the sulfated pullulan's anticoagulation. Unlike chitosan, the higher the molecular weight the longer the anticoagulation activity. This has been found with pullulan as well as other sulfated polysaccharides such as fucoidans, sulfated dextran derivatives, glycosaminoglycans from sea cucumber Suzuki, and β-1,3-glucan sulfates.[76]

Another method to create a carbohydrate mimic was creating a polymer composed of sulfated lactose-based glycopolymers.[77] Similar to the saccharide attachment to polyurethane, this method uses the disaccharide peracetyl-lactose, but instead of sulfating after attachment this procedure sulfates before polymerization. After sulfation the lactose is synthesized to be a monomer with unsaturated bonds able to be radically polymerized. Polymerization is then induced to create a polymer with a carbon chain backbone and sulfated lactose branches. The sample that produced the best anticoagulation effect had the highest molecular weight and degrees of sulfation.

These different studies show that heparin mimics can be synthesized from a variety of carbohydrates and polysaccharides and in many different ways. So long as the product contains a high degree of sulfation, i*n vitro* studies show that the sample will produce a similar response to heparin. No study of these reactants has been able to synthesize a mimic that can reduce coagulation at the same concentration as heparin. Further research in different and more specific functionalization should be done in this field to possibly create a mimic comparable to fondaparinux.

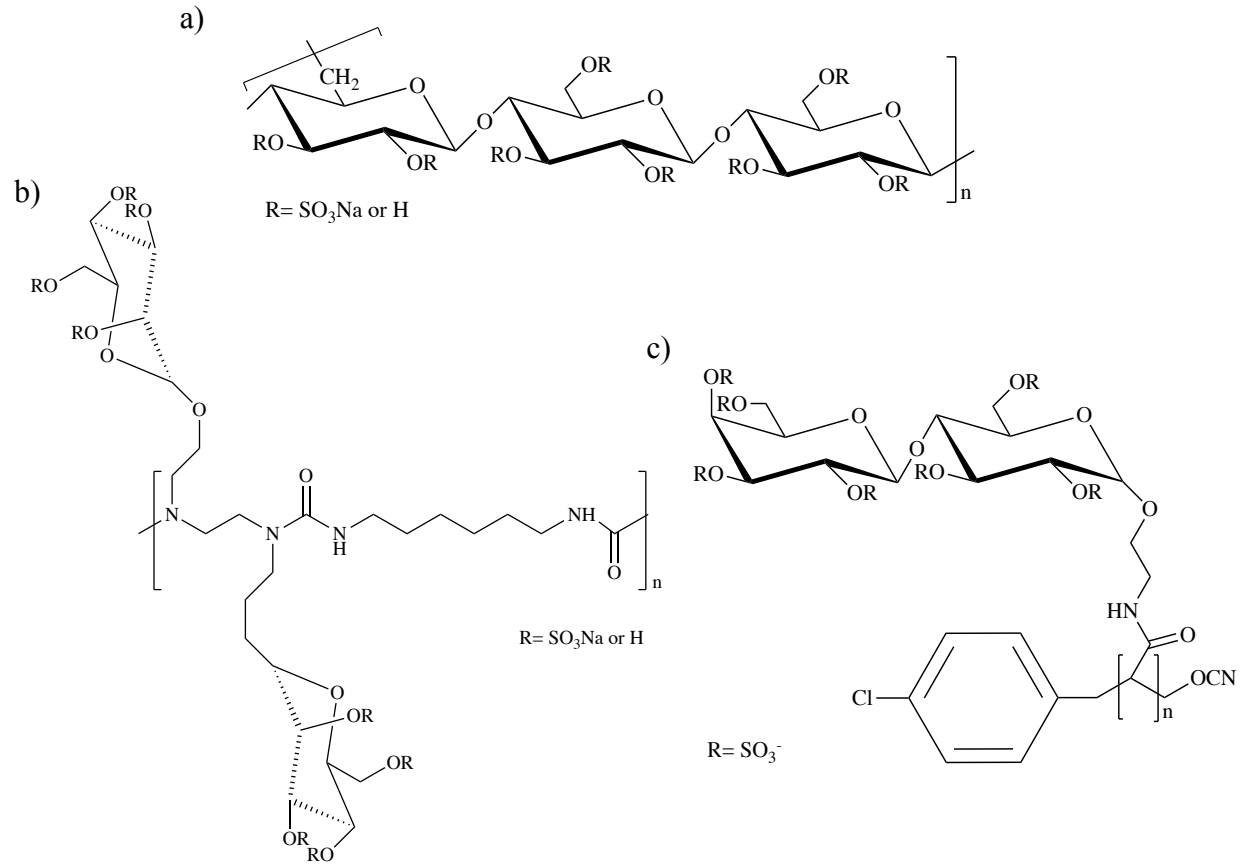

Figure 12: Several derivatives of sulfated polysaccharides a) Sulfated pullulan b) polyurethane modified with lactose then sulfated c) sulfated peracetyl-lactose *glycopolymer*

1.1.6 Vitamin K Antagonists

1.1.6.1 Warfarin

In the anticoagulant market, warfarin is the most common medication prescribed. Warfarin manages clotting by reducing the action of vitamin K. Clotting factors II, VII, IX, and X need vitamin K to be synthesized. Without its presence these factors cannot be synthesized. Warfarin interfers with the cyclic interconversion of vitamin K by inducing the inhibition of the

γ carboxylation step of vitamin K synthesis.[78-79] Warfarin is administered orally. With a half-life of 40 hours, the substance is active for a long period in the body, the effects start 12-24 hours after the initial dose. Heparin on the other hand has a rapid response time of 20-60 minutes, but only lasts 9-12 hours. The benefits of having a long active period and the ability to take it orally are why warfarin is so prevalent in the anticoagulant market. Similar to UFH, warfarin can be reversed by administering vitamin K, fresh frozen plasma, or prothrombin complex concentrates.[79]

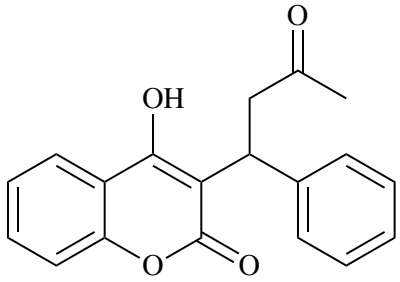

Figure 13: Structure of Warfarin

With all of the benefits from warfarin use there are also side effects. Because of its low molecular-weight, warfarin can cross the placental barrier and be a teratogenic, an agent that causes developmental malformations in an embryo or fetus.[80] Fetal bleeding is also increased because of the placental crossing of the drug. A study on pregnant women taking warfarin showed that 42% of 71 pregnancies had poor outcomes, with 32% of the patients experiencing the death of the fetus.[81]

1.1.7 Clotting Assays

1.1.7.1 Activated Partial Thromboplastin Time Assay

Activated partial thromboplastin time (aPTT), also known as kaolin-cephalin clotting time, is a clotting test used to measure the clotting time of the intrinsic pathway, which includes the conversion of factor X to Xa. LMWH and ULMWH principally employ this conversion, whereas UFH employs both the intrinsic and extrinsic pathway, which converts factor II to IIa. A normal aPTT clotting time would be 28-30 seconds.[63] A therapeutic concentration of heparin should have a clotting time of 75-115 seconds.[17] Dosage of heparin is often measured using the assay against the patient's anticoagulant free blood and multiplying its normal clotting time by 1.5-2 times through the addition of heparin.[82]

1.1.7.2 Prothrombin Time Assay

Prothrombin time (PT) looks at clotting initialized through the extrinsic pathway. The blood factors analyzed in the PT assay are factors I, II, V, VII, and X.[83] Often, this test is done to check for the blood clotting results of patients taking warfarin because vitamin K is needed to make the clotting factors. Heparin often does not change the clotting time of PT assays. Normal prothrombin times range from 8-11 seconds.[83] Similar to heparin and aPTT assays the time is adjusted to 1.5-2 times the anticoagulant free blood clotting time for warfarin dosage calculation.

1.1.7.3 Thrombin Time Assay

Thrombin time (TT) measures the conversion of fibrinogen to fibrin through the addition of bovine thrombin. Heparin use prolongs the assay result as well as abnormal fibrinogen production.[84] Other tests observing heparins impact on clotting are more commonly used than the TT assay.

1.1.8 Drawbacks of using Heparin

1.1.8.1 2008 Heparin Contamination

As discussed earlier, heparin is derived from animal tissue. This sourcing can cause impurities and lead to complications including death. In 2008 an oversulfated chondroitin sulfate (OSCS) contaminated batch of heparin affected thousands of patients in the Americas, Europe, and Asia and caused more than 200 deaths.[85] OSCS along with heparin is a GAG giving them a very similar structure (see Figure 14). Most tests conducted on heparin after manufacturing at that time were not able to differentiate OSCS from heparin, allowing the impurity to go undiscovered and into the market.

Complications caused by OSCS include low blood pressure, shortness of breath, racing heart, as well as other severe symptoms.[26, 86] The mechanism by which OSCS works is by activating the kinin-kallikrein pathway which produces anaphylatoxins and bradykinin. Anaphylatoxins generate reactions similar to anaphylaxis like facial swelling, tachycardia, and hypotension. Bradykinin, a potent vasoactive mediator, results in hypotensive side effects.

China produces more than 50% of the heparin in the world.[34] Problems like the 2008 crisis demonstrate the problems of relying disproportionately on China to manufacture the world's supply of heparin. China has low regulatory control in the food and drug industry allowing tainted drugs enter the world market. The 2008 contamination was found to be purposeful contamination to cut costs.[87] The price gap between OSCS and heparin is vast, with

OSCS only being $20 per kg and heparin $2000 per kg.[88] The creation of cheap, synthetic heparin alternatives, could generate production in the United States. U.S. production accompanied by stringent FDA regulation could also help prevent incidences like the 2008 contamination.

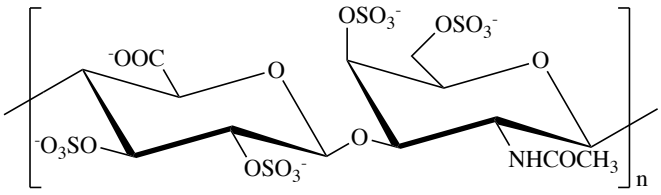

Figure 14: Structure of oversulfated chondroitin sulfate, the compound that contaminated the 2008 heparin supply

1.1.8.2 Belief Limitation

Porcine and bovine tissues are the most common tissues used to supply heparin.[11, 85] Sourcing heparin from animals introduces regulatory concerns, as demonstrated by the outbreak of mad cow disease in the 1990s, the heparin shortage of the 2000s, and the OSCS contamination crisis of 2008.[18] The derivation from animal tissue also poses religious concerns. According to the Pew Research Center in 2015 24.3% of the world is Muslim and Jewish, and 22% of the world is Hindu and Buddisht.[89] Muslims and Jews are forbidden from consuming porcine byproducts, while Hindus may not consume bovine products. Brahman Hindus and many Buddhists are vegetarians, restricting devout belivers from accepting animal based medicines. This religious conflict between drugs and belief creates a high a demand for synthetically derived heparin.

1.1.8.3 Biological Effects

Studies show that treatments using heparin can induce hemorrhage, heparin induced thrombocytopenia (HIT), hypersensitivity, elevations of aminotransferase, and osteoporosis.[11, 16, 60, 90] HIT is caused by binding to PF4, which creates a series of reactions that cause a lower platelet count and, potentially, thrombosis. Incidences of HIT are lower when patients use LMWH and almost nonexistent when using ULMWH because the shorter chain lengths have less binding affinity to PF4.[91] By controlling the molecular weight and concentration of heparin doses, HIT can be avoided.

Heparin induced osteoporosis results from heparin hindering the differentiation and function of osteoblasts, bone forming cells, as well as increasing the number of osteoclasts, bone resorbing cells.[92-94] Low bone mineral density (BMD), a value that measures the bone health and

identifies if a patient has osteoporosis, is dose and duration dependent with heparin.[94] UFH patients have more incidences of osteoporosis than patients taking LMWH and ULMWH. This is because LMWH does not decrease the amount of osteoclasts, just osteoblasts. With only bone forming cells being inhibited, the BMD remains the same in patients.[95] ULMWH have not been observed to reduce osteoblast or osteoclast activity, so they do not generate osteoporosis.[93] The mechanism behind why these compounds give this effect is not fully understood yet.

Women's blood coagulability increases while pregnant.[96] This drives women who are at a risk of blood clots to go through anticoagulant therapy during pregnancy. As mentioned earlier, the risk of miscarriages and fetal deformities increases when taking warfarin because it crosses the placenta. This influences women to take heparin for an extended period of time, which has the adverse effect of causing osteoporosis. Despite the young age of patients, one-third of heparin-treated pregnant women have a decrease in their BMD with 2.2-3.6% experiencing bone fractures.[92, 97-99] Many women experience a BMD decrease during pregnancy, but it is restored 6-12 months after breastfeeding.[95] This result needs to be further researched because there are conflicting studies on non-pregnant patients that indicate bone growth, and in turn density, does not return to its original state.[93]

1.2 Cellulose Nanocrystals

1.2.1 Cellulose

Cellulose is the most abundant, renewable, natural, and biodegradable polymer on earth, with 7.5×10^{10} tons produced annually.[2, 100-102] Many living organisms including plants, animals, and some bacteria contain cellulose. About 40% of the biomass of all organic matter, with the exception of fossil fuels, is made up of cellulose.[103] Cellulose is often referred to as a green material. Green materials are characterized as being renewable, while also often biocompatible and cost-competitive.[104] The abundance of cellulose along with the renewed interest in sustainability within today's society means it is a desirable material for consumers as well as innovators.

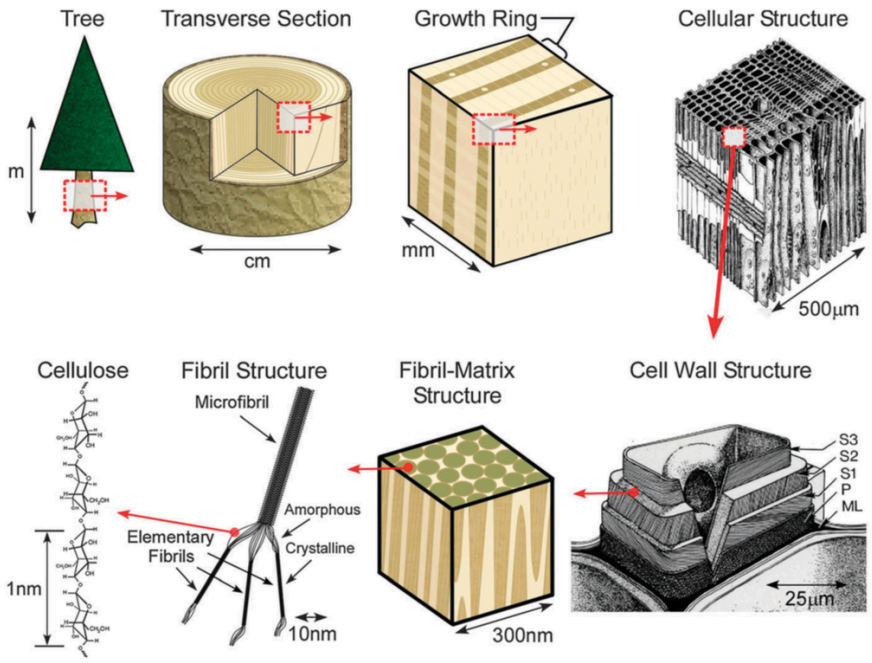

Figure 15: Hierarchial structure of wood, from the tree to the smallest subunit cellulose[1]

Polysaccharide cellulose has a linear structure made up of repeating units of anhydro-D-glucose rings, stabilized laterally by hydrogen bonds between the hydroxyl groups.[4, 101] Along with lateral stabilization, the equatorial hydroxyl groups generate hydrogen bonding between the oxygen and hydrogen groups intra- and inter- molecularly.[105] Intermolecular linking is made up of β 1-4 glycosidic bonds. Intramoleculular bonding is dictated mainly by the O3–H•••O5 bond.[4] Only one monomer is used in cellulose, β-D-glucopyranose, making it a homopolymer. Within the cellulose chain there is a 2-fold screw axis that creates symmetry along the length as seen in Figure 16 through the 1,4 linkage.[2, 105] This screw means each unit of cellulose is flipped 180° from its neighbor. Depending on the cellulose source material, the n value in Figure 16 varies from 5,000 to 7,500.[4]

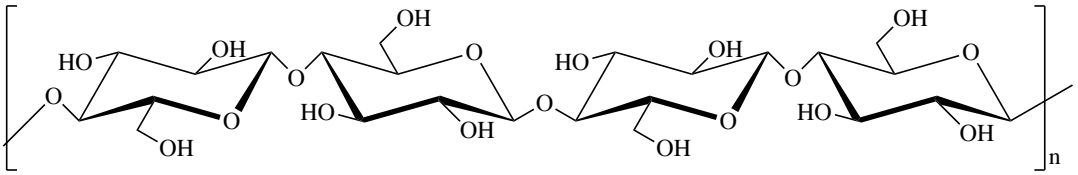

Figure 16: Cellulose structure showing the β 1-4 glycosidic bonds and 2-fold screw axis

Six different polymorphs I, II, III, IV, V, and VI compose cellulose.[106] The cellulose that is often referred to as "natural cellulose", derived from trees, plants, tunicates, algea, and bacteria, is Cellulose I. Within cellulose I there are two other polymorphs: a triclinic structure (Iα) and a

monoclinic structure (Iβ). The Iβ polymorph is dominant in cotton and wood and is more stable than the Iα polymorph.[4] All Cellulose I chains are arranged in a parallel up configuration.[106] This means that the β 1-4 glycosidic bond between each unit points in the same upward direction.

Cellulose derived from cell-walls contains a mixture composed of cellulose, lignin, hemicellulose, and pectin. Native cellulose contains both the amorphous and crystalline regions along their length or in the transverse direction.[4] The crystalline region has a higher density so when cellulose undergoes acid hydrolysis the amorphous regions break up and leave only the crystalline regions, which are the cellulose nanocrystals.[107]

1.2.2 Cellulose Nanocrystal Background and Properties

Cellulose nanocrystals (CNC), also called nanocrystalline cellulose[107-108], cellulose whiskers[106], crystalline cellulose[109], or cellulose crystallites[105], is a form of cellulose that comes from the smallest domain of the plant fiber.[110] CNCs are made up of highly ordered crystalline domains whose morphologies vary by the origin of the raw material as well as the hydrolysis performed. The hydrolysis is what removes the lignin, hemicellulose, and amorphous regions within cellulose. Longer hydrolysis reactions shift the length distributions to lower values and give a narrower polydispersity index (PDI).[107, 111] Wood CNCs range from 3-5 nm in width and 100-300 nm in length with a crystallinity of 50-83%.[2, 112] Depending on the source, the rod-like structure changes. For example bacterial and tunicates cellulose chains have a twisted-ribbon geometry.[108] The effect of this different geometry on the mechanical and physical properties of CNCs has not been studied yet.

Table 2: Dimensions of CNCs from difference sources observed through TEM imaging

Source	Length (nm)	Width (nm)	Crystallinity (%)	References
Wood	100-300	3-5	50-83	2, 107-108, 112
Cotton	100-350	5-15	55-80	2, 107, 112-114
Tunicate	100-4000	10-30	85-100	2, 4, 107, 112
Bacterial	100-1000	10-50	>70	2, 107, 112, 115-116
Algal (Valonia)	>1000	10-20	95	2, 107, 112, 117

The abundance of hydroxyl groups on cellulose allows for easy chemical modification. Modifications that have been examined include esterification, etherification, oxidation, silylation, polymer grafting, among others.[2] Even though there is an abundance of hydroxyl groups on

CNCs only half are accessible and can react.[2] The other half are buried within the crystalline particle. Out of all the hydroxyl groups on CNC the most reactive and commonly functionalized is the one in the sixth position.[107] The reactiveness of the position of each hydroxyl group is visualized in Figure 17. The introduction of new functional groups is often done to introduce different electrostatic charges on the cellulose to alter dispersion or tune the surface energy characteristics.[2]

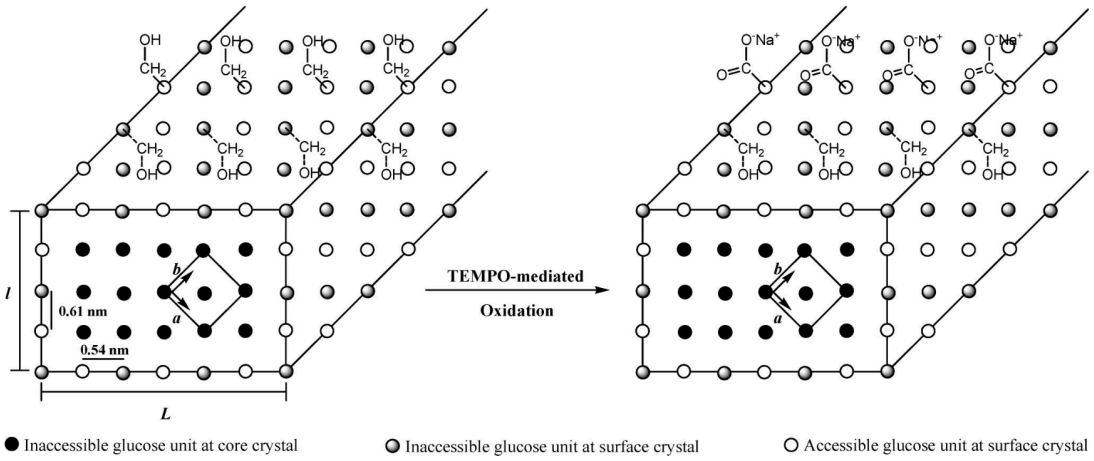

Figure 17: Visualization of hydroxyl groups able to be functionalized on CNCs, using the example of TEMPO mediated oxidation[2]

Development of materials derived from CNCs has increased dramatically in the past decade because of their desirable properties such as their nanoscale dimension, exceptional mechanical properties, high aspect ratio, low density, low toxicity, low thermal expansion, and unique morphology.[2, 4, 107, 112, 118-120] CNC materials are able to create specific functionalization as well as ideal strength properties.

1.2.3 CNC Production from Raw Materials

Raw materials like wood, cotton, bacteria, etc. are used to manufacture CNCs. First, cellulose must be extracted from the cell walls from the stem, leaf, or fruit. The world's production of wood is degrees of magnitude larger than that of all other sources of cellulose so their isolation will be focused on. CNCs are extracted from the terminal enzyme complexes within the cell walls of wood. Most of the matrix, composed of lignin, hemicellulose, and impurities, must be removed to create "purified wood".[4] Different methods of removing the matrix dictate the morphology, aspect ratio, crystallinity, and crystal structure of the CNCs.[4] After the removal of the matrix only the amorphous and crystalline regions remain in the cellulose fiber. The fiber is then bleached and put into solution to be ready for hydrolysis.

1.2.3.1 Acid Hydrolysis

To isolate the crystalline regions within cellulose the three most common techniques used are mechanical treatment, acid hydrolysis, or enzymatic hydrolysis. The most well known, efficient, and widely used of the three is acid hydrolysis, so this is what will be focused on.[118] Isolating CNCs from cellulose using acid hydrolysis yields a highly crystalline rod-like or whisker shaped product with colloidal dimensions. The disordered amorphous regions of cellulose fibers are removed, leaving only single well-defined crystals.[118]

Common acids used in this procedure include sulfuric[112], phosphoric[121], and hydrochloric[122] acid. Using different acids creates a very low concentration of surface functionalization on the CNCs. For sulfuric, phosphoric, and hydrochloric acid hydrolysis, the functional groups added are $-SO_3^-$, $-PO_3^-$ and –H respectively. The $-SO_3^-$ groups given during sulfuric acid hydrolysis gives CNCs a similar functional group to heparin. It also allows suspensions of CNCs to form an ordered phase at a concentration above a critical value. Phosphoric and hydrochloric acid have not been able to create the same effect.[123] The negatively charged sulfate groups produce a perfectly uniform dispersion through electrostatic repulsions.[2]

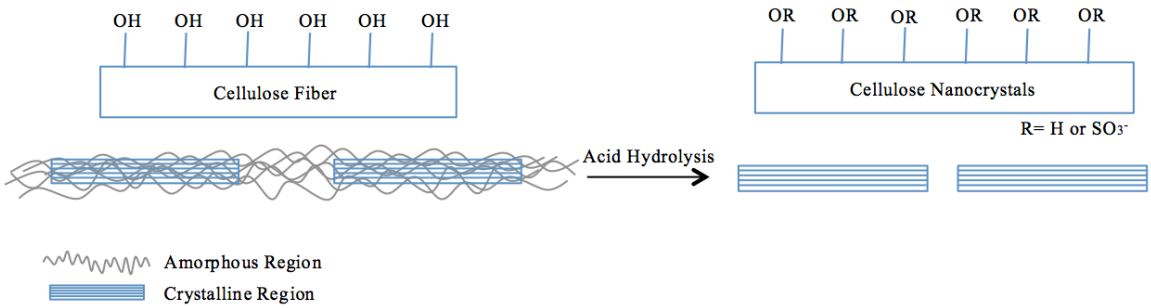

Figure 18: A modified version of Moon and Ng's visualization of the acid hydrolysis reaction on removal of the amorphous regions in CNC [3-4]

When conducting acid hydrolysis the concentration of acid used needs to be strong enough to break the glycosidic bonds but weak enough to not completely hydrolyze the chain into glucose units. The best concentration range for sulfuric acid hydrolysis has been found to be around 60-70%.[123] Using sulfuric acid as the hydrolyzing agent brings a net negative charge (30-90 mmol/kg) on to the surface of the CNCs, which allows electrostatic stabilization in an aqueous media.[121, 124] In order to get CNCs with a minimal charge on the surface, hydrochloric acid is used.[112] This lack of charge causes the CNCs to not have the ability to disperse readily and flocculate.[107]

The procedure to get rod-like CNCs involves using two acid-to-pulp ratios of cellulose and 64% w/w sulfuric acid and stirring for 45-60 minutes at 45 °C. To quench the reaction a 10-fold dilution of water is added. The product is centrifuged against water several times to get an acid-free precipitant. This precipitant is dialyzed against water for 5 days.[124] The dialysis solution is then centrifuged again and the remaining sediment is sonicated in an ice bath. The residual electrolyte is removed from the sediment through filtration on 8 μm then 1μm membranes and a mixed bed resin.[111, 118] The filtered product gives the final crystalline cellulose solution.

1.2.4 Surface Modification of CNCs

1.2.4.1 TEMPO Mediated Oxidation

The green reaction of using 2,2,6,6-tetramethylpiperidine-1-oxyl (TEMPO) as a nitroxyl free radial catalyzes the oxidant hypochlorite to specifically oxidize the primary hydroxyl group on CNCs. This reaction is considered 'green' because the reactants uses water as the solvent. The morphology of the CNCs after the reaction in able to be maintained, but with a high enough sodium hypochlorite concentration excessive oxidation may occur and the amorphous regions are further degraded.[107]

Along with sulfuric acid hydrolysis TEMPO oxidation generates more negatively charged functional groups on the surface of CNCs. This allows better dispersion in water due to electrostatic stabilization. Further surface modification can be more easily done with the dispersion of TEMPO CNCs than non-functionalized CNCs.[107]

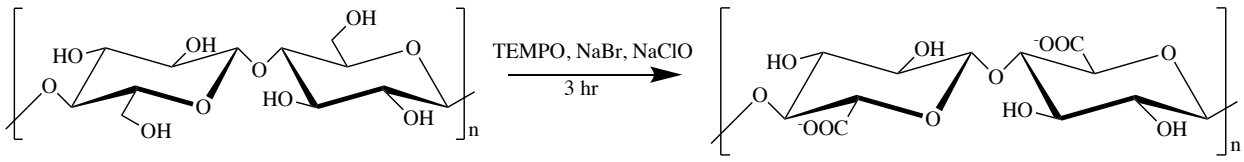

Figure 19: TEMPO oxidation of CNCs

1.2.4.2 Sulfonation of CNCs

CNCs are able to replace the hydroxyl group with a sulfate group through the reaction with sulfur trioxide amine complex and a solvent.[125] These complexes are used because once in the solvent the complex breaks apart to form a sulfur trioxide radical that reacts to switch with the proton on the hydroxyl group. This 'switching' occurs because sulfur trioxide is an extremely electrophilic reagent and the oxygen in the hydroxyl acts as a nucleophile.[126] The complex is used over just sulfur trioxide because it is highly reactive and needs to be stabilized. Formation

of the complex is done by attaching the sulfur trioxide to a tertiary amine. Common chemicals used as the amine donor to the complex are dimethylformamide, trimethylamine, N,N-dimethylaniline, and pyridine.

The degree of sulfonation depends on several variables but most importantly the sulfating agent, medium, reaction time and temperature, and molar ratio of reactants.[75] A study showed how several of these factors affected the degree of sulfation when using sulfur pyridine trioxide complex as the sulfating agent.[127] By increasing the temperature, time, and mole ratio of reactant they were able to alter the degrees of sulfation. The use of pyridine over dimethylformamide (DMF) as the solvent allowed the sample to be heated up to a higher temperature, producing a higher sulfated product. Studies have also exhibited that if the mole ratio is increased from 1:4 to 1:8 at 40 °C for 48 hours the degree of sulfation rises from 1.88 to 2.46.[66] Even with this high degree of sulfation, not all the hydroxyl groups present on the CNCs are sulfated. Some are left unmodified. This model is based on chitin, but the basic hydroxyl functional group alteration and backbone structure is the same in cellulose.

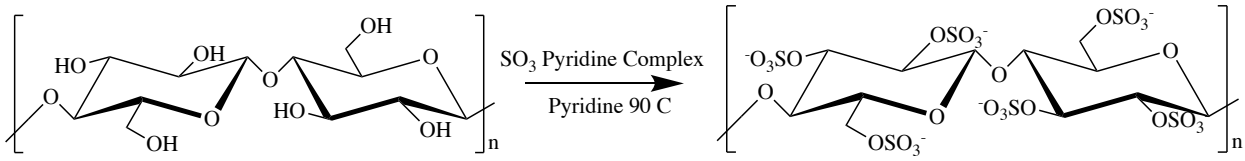

Figure 20: Sulfation reaction of cellulose nanocrystals using sulfur pyridine trioxide complex and a pyridine solvent

1.3 Biomaterials

1.3.1 CNC Biomaterials

Cellulose nanocrystals are a great addition to biomaterials because of their properties described in section 1.2.2. The ability to be biocompatible, biodegradable, low cost, and very functionally reactive gives them attributes that are hard to replicate.[107, 128] A possible negative result is that CNCs are able to be metabolized by some microorganisms, but humans likely do not have this ability. This is due to humans not having cellulose-specific enzymes that are needed to digest cellulose. This idea has not been studied, but when incorporating CNCs into a material they should not be released into the body.

CNCs can be incorporated in materials through casting-evaporation, freeze-drying/molding, and extrusion. Out of these techniques casting-evaporation produces the best mechanical properties. When casting-evaporating CNCs with a polymer unlike most composites

the matrix/filler interaction is not favored. The hydrogen-bonded percolating networks that are induced by CNCs above the percolation threshold cause this phenomenon and enable the amazing reinforcing effects CNCs have on their composite.[129] The order of CNCs reinforcing efficiency in a nanocomposite casting techniques goes from evaporation, to hot pressing, then extrusion, from most efficient to least.[2] The evaporation process allows CNCs time to create and interconnect the essential percolation network for the composites mechanical properties to be enhanced.

1.3.2 Protein Adsorption and Adhesion on Biomaterials

Protein adhesion and activation are important factors to consider when making a biomedical material, especially for blood-contacting materials. Once a material comes in contact with blood protein adsorption, platelet adhesion and activation, coagulation, and thrombosis are stimulated. Proteins that can adsorb to the surface through the blood are fibronectin, vitronectin, von Willebrand factor, albumin, immunoglobulins and fibrinogen, with fibrinogen inducing clotting the greatest.[6] Through reduction or removal of protein adsorption and adhesion, platelet adhesion should also be eliminated. Materials and their surface properties dictate the response and its magnitude. Figure 21 shows how the presence of several different elements can develop a biological response. Surface property factors that influence adhesion and activation are topography, composition, hydrophobicity, heterogeneity, and charge.

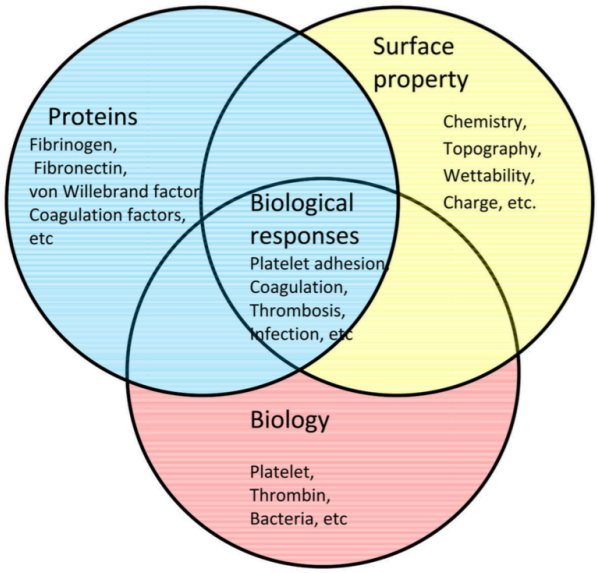

Figure 21: The effects of different properties on blood compatibility[6]

Hydrophobic materials have been shown to produce more protein adsorption than hydrophilic materials. Hydrophilic surfaces reduce protein adhesion because they are strongly bound to water molecules making it difficult for proteins to displace the bonding. Hydrophobic surfaces induce protein adhesion through 'hydrophobic hydration', which stimulates water molecules to bind to the surface through van der Waal forces. Proteins then adsorb to water molecules creating a protein-water-polymer layer. When this layer forms the water molecule in between the protein and polymer is replaced by water on the surface of the protein. This creates a conformational change where the hydrophobic portion of the protein then becomes available and binds to the material.[130]

Functionalization of surfaces can also affect protein adsorption and alter the materials overall hydrophobicity. Comparing methyl, amine, hydroxyl, and carboxyl groups adhesion forces against blood plasma proteins methyl by far showed the greatest and carboxyl groups showed the lowest.[131] Table 3 shows several other features that biomaterial surfaces can have that effect protein adhesion. Materials that resist protein adhesion the best are often hydrophilic, neutral charged, contain hydrogen-bond acceptors, and no hydrogen-bond donators.[6]

Table 3: Material surface properties that effect protein adhesion[132]

Feature	Effect
Topography	More topography results in a larger surface area and in effect more protein interactions
Composition	Surface functionalization controls the type of intermolecular forces the surface has with proteins
Hydrophobicity	Proteins bind more readily to hydrophobic surfaces
Heterogeneity	Differences in surface characteristics can influence portions of the material to produce diverse protein interactions
Potential	Surface potential can alter the distribution of ions in solution and proteins interactions

1.3.3 Hemodialysis

1.3.3.1 Background

More than 1.4 million patients world-wide have end-stage renal disease (ESRD).[133] To keep their body from shutting down, these patients must undergo hemodialysis (HD) to remove toxins and excess fluid from of their bloodstream. HD is when blood continuously flows from

the body to the extracorporeal circuit (EC) and back. In the EC blood is filtered through a membrane that extracts waste and fluid. According to the National Kidney Foundation, patients undergo dialysis on average three times per week for four hours.[134] This number of treatments varies depending on the condition of a patient's kidney.

The EC is made up of the arterial cannula, venous cannula, peristaltic blood pump, dialyzer, and many other components.[135] Clotting in the EC is influenced by blood exposure to air, turbulent flow in the circuit, and blood components coming in contact with dialysis tubing.[136-137] Exposure to air and flow of the system can be reduced in modern HD techniques. When blood comes in contact with the dialyzer, it stimulates the coagulation cascade through the extrinsic pathway by activating leukocytes.[133] To counteract the blood components creating a clot, heparin is lined along the dialysis surface and/or administered intravenously. LMWH can be administered subcutaneously for clot prevention, but lining dialysis tubing with it has not yet been approved in the United States.[137] The most common material used for blood lines is polyvinyl chloride (PVC) along with the softener di-(2-ethylhexy)-phthalate (DEHP).[135]

All the negative side effects that occur from heparin administration can also take place when it is used for HD. With HD patients' constant need for dialysis treatment, heparin and its potential side effects can be amplified. HD patients are in a state where their kidneys can barely function so additional medical complications could bring their body closer to failure. Because of patients' reduced kidney function and the fact that 50% of UFH is cleared through the kidneys, the half-life of heparin is increased in ESRD patients. [133] The half-life of heparin is extended from 30 minutes in a patient with normal kidney function to 1 hour in an ESRD patient.[133] This can cause heparin to build up in the body and further complications.

Currently, patients who are at a high risk of bleeding have the option to participate in anticoagulant free HD or anticoagulant HD. Anticoagulant free HD is a more complicated treatment, but, may be chosen because, if a high bleeding risk patient is exposed to heparin, their risk of hemorrhaging increases. During this procedure the tubing that comes in contact with blood needs to be changed more often because of the formation of clots during the procedure. With a material that resists clotting no substance will need to be metabolized by the body, reducing the strain on HD patient's kidneys.

1.3.3.2 Polyvinyl Chloride Material

A common dialysis tubing material used is polyvinyl chloride (PVC) plasticized with di(2-ethyl hexyl)phthalate (DEHP). This material has been used for several functions other than dialysis tubing such as flexible tubing for infusers and blood bags. Plasticized PVC is commonly chosen for these materials because of its flexibility, toughness, optical transparency, weldability, and very low cost.[138] DEHP is commonly used in blood contacting devices because its release enables better preservation of red blood cells when stored.[138] A problem with this material is that DEHP has shown to leech out of PVC at a rate whose concentration values are close to that of rats LD_{50}. Lethal does (LD_{50}) is the dose, or amount, that must be administered to kill 50 percent of the population tested.

A study quantified the amount DEHP that leeches from blood bags to be 0.1 mg/mL blood after 21 days.[139] With an oral LD_{50} for DEHP in rats being > 20 g/kg and the lowest no-observed-adverse-effect-level (NOAEL) for kidney toxicity in rats is 29-36 mg/kg/day this leeching value well surpasses the limit.[140] Current PVC tubing on the market shows that several manufacturers specifically state the product is DEHP-free because of these potentially harmful effects. Even with all these problems Solloum states that DEHP is still the most widely used plasticizer for blood bag applications.[138]

PVC's chemical properties activate protein adhesion and adsorption. By removing proteins from the system through attachment to the PVC surface, the body, which is already in a high stress state from dialysis, is deprived of essential blood proteins. This deprivation can cause decreased brain size, cognitive function, altered fat distribution, lethargy, depression, and immunosuppression.[141] PVC does not inhibit coagulation or help limit it even though it is the most commonly used material for these processes.

1.3.3.3 Polyethersulfone Material

Recently, polyethyersulfone (PES) has gained popularity as a polymer for clinical hemodialysis. Its stability and mechanical properties with great oxidative, thermal, and hydrolytic stability and a Young's modulus of 32.7 MPa makes PES an attractive alternative.[142-143] A limiting factor to using PES hemodialysis is its hydrophobic nature. When hydrophobic materials come in contact with blood, they stimulate protein absorption as well as platelet adhesion and activation. Many researchers are looking at alteration of the material through composites to reduced or eliminate its clotting properties.

Several studies have looked into using PES as a composite in heparin-mimicking membranes for dialysis.[144] The heparin mimicking membranes were made through spin-coating PES with carbon nanotubes that were synthesized to have domains similar to heparin. These membranes showed decreased platelet adhesion as well as high aPTT times. The best anticoagulation result was created by the sample with the highest sulfate group concentration.

2 Statement of Work

Current blood-contacting materials used during HD do not actively inhibit clots from forming. This is why patients typically need heparin administered during their HD treatments. To reduce or eliminate the need for heparin therapy, a blood-contacting material would either need to have the characteristics similar to a blood vessel and/or inhibit the coagulation cascade. Hydrophilic surfaces, negatively charged functional groups, and topography mimicking blood vessels create the ideal *ex vivo* material environment for blood flow.

This thesis is based upon the hypothesis that current HD treatment can be improved upon by reducing the possible complications due to heparin by altering the blood-contacting portion of the dialysis tubing to have anticlotting abilities similar to that of heparin. These abilities are stimulated by the presence of functionalized CNCs. Using CNCs in a composite like the one proposed is beneficial because they contained hydroxyl groups that can be easily functionalized while increasing mechanical properties. Other heparin mimics focus on replacing heparin in its solubilized form. We are taking a different approach and placing it in a material. The initial research that has been done during this project mainly focuses on the functionalized CNCs in solution to see if the proposal is plausible. Further research will then take these CNCs and add them to a composite which presents the CNCs on the blood-contacting portion of the material.

Different CNC functionalization's that mimic the antithrombin binding region on heparin were analyzed to see which best inhibits coagulation through three different blood tests: activated partial thromboplastin time, thrombin time, and prothrombin time. These three tests show where in the coagulation cascade the material inhibits clotting factors, the intrinsic, extrinsic, or common pathway. All these tests were conducted with CNCs in solution. Platelet fixing was done on materials. The composition selected for this testing was a 30 wt% CNC/polyurethane composite. This test showed if platelets were able to adhere to the material or not.

3 Paper: Synthesizing a Heparin Mimic Material Derived from Cellulose Nanocrystals

3.1 Introduction

Anticoagulants are chemically synthesized, naturally occurring, or semi-synthetic substances that reduce coagulation through the suppression of clotting factors. The reduction of coagulation can reduce, treat, or prevent the risk of blood clots breaking off and traveling through the bloodstream to organs, resulting in strokes, pulmonary embolisms, or deep vein thrombosis, as well as prevent blood from clotting during surgeries or dialysis treatment. A wide range of blood-related operations, devices, and treatments can now be accomplished through the use of anticoagulants. Medical uses range from thrombosis, embolisms, kidney dialysis, cardiopulmonary bypass, and the prevention of clotting during surgery.[10-11] Materials that are being investigated have surface chemistry which mimics that of heparin. The structures are covalently bound to the material so they do not diffuse into the system and produce sytemic anticoagulation.

One of the most widely used and efficient anticoagulants is heparin, with thirty percent of hospital patients exposed to it in the United States.[12-14] Heparin is a linear, sulfated, and highly negatively charged polysaccharide (~75 mmol negative charge density/kg) biosynthesized in the Golgi of mast cells.[9, 15-18] The basic structure of heparin is composed of α-1,4 linked uronic acid and D-glucosamine with an average molecular weight of 15,000-19,000 Da and a polydispersity index of 1.1-1.6.[11, 26-27] The high negative charge of heparin mainly derives from its sulfate functional groups which correspond to about 2.5-2.7 sulfate groups per disaccharide unit.[9, 16, 29]

To restrict coagulation, a heparin chain, with a minimum length of 18 residues, interacts with the serpin plasma cofactor antithrombin (AT).[12, 15, 28-30] This interaction causes a conformational change in AT that creates a tertiary complex between AT, factor Xa, and thrombin (factor IIa). Clotting factors Xa and thrombin are therefore removed from interacting with the system, disrumpting the clotting cascade.

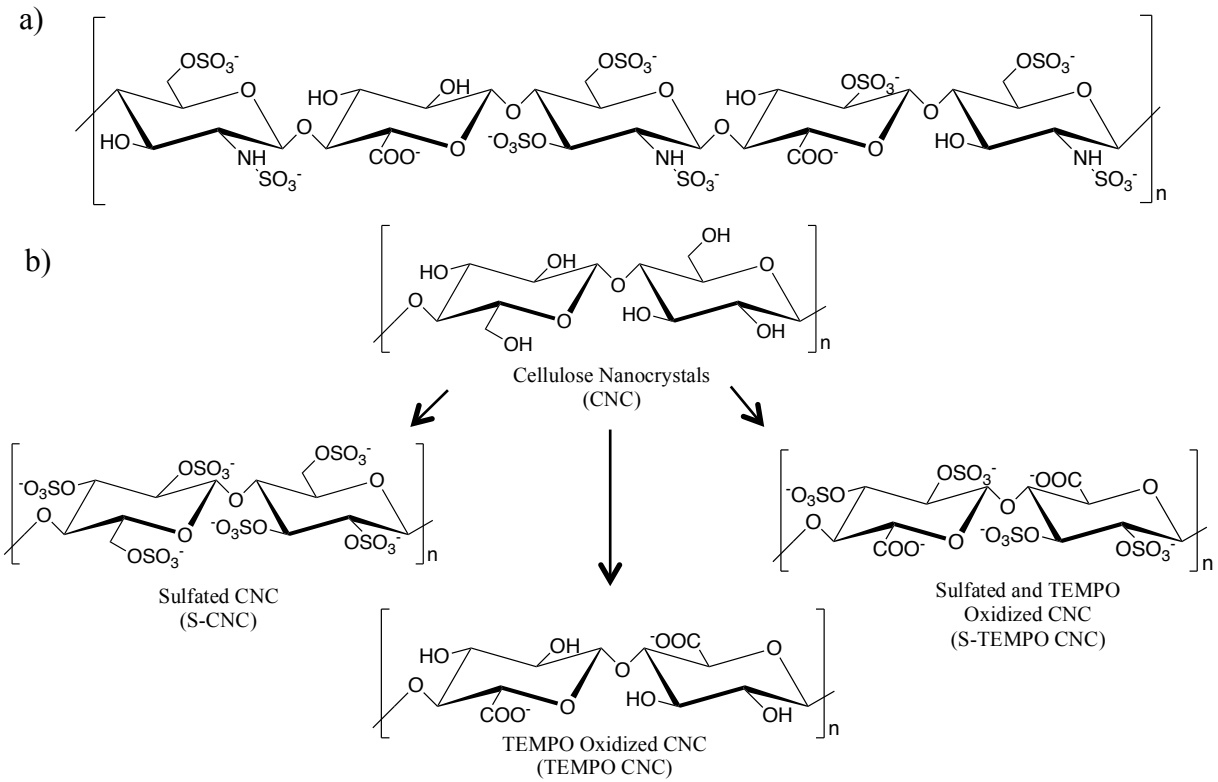

Figure 1: CNCs structure similarity to the ATBR make it a good template for functionalization to create a chemical structure comparable enough to have the ability to inhibit coagulation a) Antithrombin binding region within heparin b) Different heparin mimicing CNC functionalizations produced through synthesis

This ATBR is mimicked in the ultra-low-molecular-weight heparin, fondaparinux (Arixtra). Fondaparinux inhibits coagulation well, but its synthetic yield is only about 0.1% and takes ~55 steps.[63] With fondaparinux's synthesis producing such a low yield and having so many steps, the drug remains very expensive to produce, and, as a result, it is not readily available to the public. By utilizing cellulose nanocrystals, basic glucose structure and reactive hydroxyl groups, a cheaper alternative to fondaparinux can be made.

Cellulose nanocrystals (CNC) also called nanocrystalline cellulose[107-108], cellulose nanowhiskers[106], crystalline cellulose[109], or cellulose crystallites[105] are a form of cellulose made up of highly ordered crystalline domains. Wood CNCs range from 3-5 nm in width and 100-300 nm in length with a crystallinity of 50-83%.[2, 112] Materials derived from CNCs are being developed more often because of their desirable properties such as their nanoscale dimension, exceptional mechanical properties, high aspect ratios, low density, low toxicity, low thermal expansion, and unique morphology.[2, 4, 107, 112, 118-120, 145]

Due to the wealth of hydroxyl groups on cellulose surface, chemical modification is easily done. Though there is an abundance of hydroxyl groups on CNCs, only half are accessible and can react.[2] By utilizing CNCs hydroxyl group reactivity and favorable mechanical properties, materials created will have both specific functionalization capabilities as well as ideal strength properties.

Compared to past work forming a CNC anticoagulant material, ours will be more specific to mimicking heparin's structure and looking at which functional group contributes the most to anticoagulation on CNCs.[146] Work done by Ehmann shows CNCs that were hydrolyzed from cellulose by sulfuric acid, with no further processing, inhibit coagulation of blood when compared to a control of polyethyleneimine (PEI). This study did not fully characterize the CNCs and only measured coagulation using glass slips and a microscope. By functionalizing CNCs and characterizing them through energy dispersive x-ray (EDS), attenuated total reflectance Fourier-transform infrared spectroscopy (ATR-FTIR), and conductometric titrations, we were able to more fully characterize the charge and structure of the CNCs. Coagulation assays that are usually done for heparin testing, activated partial thromboplastin time (aPTT), prothrombin time (PT), and thrombin time (TT), were carried out on our samples to determine how their anticoagulation profiles compare to heparin and other heparin mimics made.

Our aim was to create a CNC film that would have the ability to inhibit platelet activation and aggregation, contain great mechanical properties, while also reducing coagulation. The applications for this material could range from dialysis tubing to catheters to blood collection and storage bags.

3.2 Experimental

3.2.1 Materials

Sodium hydroxide solution, dichloromethane, ethyl acetate, and hydrochloric acid solution were obtained from Fisher Scientific. Texin RxT70A polyurethane was purchased from Covestro. All other chemicals were purchased from Sigma-Aldrich. All materials were used without further modifications.

Dried cellulose nanocrystals (CNCs) and an 11.8 wt% slurry of CNCs were purchased from the University of Maine Forest Products Labs. These CNC samples were extracted from wood pulp using sulfuric acid hydrolysis. Thromboplastin was acquired from Biopool. Bovine alpha-thrombin was purchased from Enzyme Research Laboratories. Blood was collected by the

Hoxworth Blood Center at the University of Cincinnati with no identifying information. Blood drawn on the day of the experiments was immediately used to make platelet rich plasma (PRP), and the PRP was purchased for research use. Within 2 hours of preparation the plasma was used in the reported experiments. Platelet poor plasma was prepared by centrifuging platelet rich plasma for 25 total minutes at ambient temperature. After 15 minutes of centrifugation at 1500 x g three-fourths of the supernatant was removed and centrifuged again for 10 minutes at 1500 x g to minimize the platelets remaining in the platelet poor plasma (PPP).

3.2.2 Methods

3.2.2.1 Sulfonation of Cellulose Nanocrystals (S-CNC)

Huang's sulfonating carbohydrates procedure was modified for CNC sulfonation.[63] An 8:1 mole ratio of sulfur pyridine trioxide complex to CNC-1, respectively, was added to a flame-dried flask. The flask was evacuated and refilled with nitrogen three times before adding anhydrous pyridine. The solution was heated to 90 °C for 16-36 hours. Saturated sodium bicarbonate was added until the pH was 8. The solution was then dialyzed until the pH of the water stayed at 7 after 24 hours then lyophilized to acquire a white powder.

3.2.2.2 TEMPO Oxidation of Cellulose Nanocrystals (TEMPO CNC)

This procedure is a modified version of Hoeng's process.[147] CNC-1 (11.8 g, 0.205 mol) were suspended in deionized (DI) water (775 mL) of water TEMPO (325 mg, 2.08 mmol), NaBr (3.564 g, 0.35 mol), and water was stirred together for 30 minutes. The CNC and TEMPO/NaBr solutions were mixed together before drop wise adding NaClO (66 g, 0.89 mol). The solution's pH was maintained at 10 for 3 hours using sodium hydroxide (0.05 M). Afterward, the reaction was quenched with ethanol. The solution was dialyzed and lyophilized to attain a white powder.

3.2.2.3 Sulfonation of TEMPO CNCs (S-TEMPO CNC)

The same sulfonation method as shown previously was used except with TEMPO oxidized CNCs as the reactant. The molecular-weight change in the CNCs was accounted for in the process.

3.2.2.4 Preparation of CNC/Polyurethane Films

Varying CNC types (TEMPO CNC, S-TEMPO CNC, S-CNC) were sonicated in DMF to make a 16 mg/mL solution. Polyurethane was then measured out to make a 50 mg/mL solution with DMF. The solutions were then mixed together to make a 30:70 wt % CNC:PU material. The solution is then added to a Teflon dish and heated for about 8 hours at 90 °C. The films were

removed from the Teflon dishes and heated in an oven at 90 °C to remove all residual DMF in the film.

3.2.2.5 Energy-dispersive X-ray Spectroscopy (EDS)

Energy-dispersive X-ray Spectroscopy was conducted using a scanning electron microscope, the FEI Quanta 600 FEG, at the Nanoscale Characterization and Fabrication Laboratory (NCFL) at Virginia Tech. Samples were coated with 10 nm of high-resolution iridium before imaging. Elements quantified were carbon, oxygen, sulfur, and sodium.

3.2.2.6 Conductometric Titrations

Conductometric titrations were performed using the Metrohm 905 Titrando autotitrator equipped with 856 conductivity module. Tiamo software was used to collect and compile the data. CNCs and functionalized CNCs were dispersed in distilled water using either stirring or sonication. Sodium chloride and hydrochloric acid was added to the solution and stirred until the pH remained constant. The titration vessel was filled with nitrogen gas immediately before the titration. Sodium hydroxide was the titrant used to determine the surface charge density. The titration gave a V- or U-shaped curve that was then plotted and fitted to give three lines; HCl titration, CNC titration, excess NaOH. The lines were then used to calculate the number of negatively charged functional groups on the CNCs. The method used to calculate the values from the titration was based on previous work by Espinosa.[148]

3.2.2.7 Transition Electron Microscopy

Transition electron microscopy was conducted using the JEOL 2100 TEM at the Nanoscale Characterization and Fabrication Laboratory. On a silicon monoxide-coated Formvar grid a droplet of 0.001 mg/mL CNC sample was incubated for one minute before being stained with NanoVan and rinsed with DI water.

3.2.2.8 Attenuated Total Reflectance Fourier-Transform Infrared Spectroscopy

ATR-FTIR spectra were obtained on a Varian 670 FT-IR spectrometer equipped with a diamond Specac Golden Gate attachment. All spectra were collected with an average of 64 scans for powdered samples and were recorded from 4000 to 500 cm^{-1} with 4 cm^{-1} resolution. A background spectrum collected on ambient air was subtracted from the sample spectra. The spectra were not corrected for the depth of wavelength penetration.

3.2.2.9 Blood Clotting Studies

Serial dilutions of CNC, TEMPO CNC, S-CNC, and S-TEMPO CNC were made starting at 5 mg/mL using pH 7.35 HEPES as the solvent. Each sample was vortexed until in solution. Once in solution the samples were serial diluted against plasma to create a plasma/dilute sample/buffer solution. Control samples only contained the buffer solution.

3.2.2.10 Activated Thromboplastin Time Assay

Activated partial thromboplastin times were initiated using PPP through Sta-PTT reagent on a STA-Hemostasis Analyzer (Diagnostica Stago). Samples were added intothe plasma at 1:10 volume ratio. If no clot formed by 300 seconds then it was assumed a clot would not form in a timely manner.

3.2.2.11 Thrombin Time Assay

A 20 U/mL thrombin solution and a 400 mM $CaCl_2$ solution was made in pH 7.35 HEPES-buffered saline. This thrombin/$CaCl_2$/buffer solution was kept on ice and the plasma/dilute sample/buffer solution was placed in a 37 °C bath. After thermal equilibrium, the thrombin solution was added to the plasma solution at a 1:10 ratio, respectively. The sample was pipetted up and down to initiate the mixing beginning the coagulation process, and a stopwatch was started. Until the sample clotted it was agitated with a toothpick. Once a clot formed the time was recorded. If the sample did not clot by 75 seconds, then it was assumed a clot would not form in a timely manner.

3.2.2.12 Prothrombin Ttime Assay

In a 37 °C bath thromboplastin and plasma/dilute sample/buffer solution were warmed. Once warmed, the two solutions were mixed in a 1:1 ratio. The sample was pipetted up and down to initiate the mixing starting the coagulation, and a stopwatch was started at this time. Until the sample clotted it was agitated with a toothpick. Once a clot formed, the time was recorded. If the sample did not clot by 75 seconds, then it was assumed a clot would not form in a timely manner.

3.2.2.13 Platelet Adhesion to Materials

The polyurethane/CNC samples were cut into 3 mm x 3 mm pieces. Each piece was placed into a 24-well tissue culture plate. From a 1 M $CaCl_2$ stock solution plasma rich plasma (PRP) or plasma poor plasma (PPP) was made to have a final concentration of 2 mM $CaCl_2$. Duplicate samples were submerged into either 1 mL of $CaCl_2$/PRP or in 1 mL $CaCl_2$/PPP. The plate was

then incubated at 37 °C for 1 hour. Afterwards, the plasma solution was carefully removed by aspiration and the samples were washed three times with Tris-buffered saline (TBS) solution. To chemically fix the adhered platelets on the samples, 1 mL of 2 % glutaraldehyde/TBS solution was added to each well. Samples were then incubated for 30 minutes. After fixation, the samples were carefully washed twice with 1 mL TBS, and then with a series of solutions with increasing ethanol concentrations (50 %, 70 %, 90 %, 100 %). Samples were dried in a vacuum desiccator before being coated with iridium for imaging using a scanning electron microscope.

3.3 Results and Discussion

The CNC samples that were not functionalized were named CNC-1 and CNC-2. Dried CNCs from the University of Maine were named CNC-1 and the University of Maine 11.8 wt% slurry was named CNC-2.

3.3.1 Energy-dispersive X-ray Spectroscopy (EDS) Characterization

Energy-dispersive X-ray spectroscopy (EDS) was used to qualitatively quantify the elements present in the bulk of the CNC sample. EDS permits characterization of CNCs using less than a mg of sample. The elements identified were carbon, oxygen, sodium, and sulfur. Hydrogen and nitrogen were not examined because EDS is unable to qualitatively identifiy them due to the limitation of the instrument .[149] This data also shows the percent of each element in the region being examined on the sample. These results demonstrated if there was a large or small amount of sulfur present.

Sulfated CNC (S-CNC) samples showed a much larger sulfur concentration percent than that of any of the other samples, see Table 1. Along with the higher levels of sulfur there was also a corresponding increase in sodium. This indicates that the added sulfur creates a negative charge density and the sodium is ionically bonded to stabilize the compound. This was also shown in the TEMPO CNC sample, suggesting that the carboxyl groups substituted for the primary hydroxyl groups on the original CNC.

An additional peak was identified as iridium, the coating used. This peak can also represents phosphorus as well as iridium. To rule this out, a sample was coated in gold and analyzed by EDS, and no quantifiable phosphorus peaks were observed.

Table 1: Elemental compositions of plain and functionalized CNCs measured by energy dispersive x-ray (EDS). The large increase in sulfur concentration that is synthetically added to the S-CNC and S-TEMPO CNC indicates that the sample was successfully functionalized

	Carbon (%)	Oxygen (%)	Sodium (%)	Sulfur (%)
CNC-1	61 ± 13	35 ± 13	1 ± 1	2 ± 1
CNC-2	56 ± 11	43 ± 11	0.6 ± 0.4	0.8 ± 0.3
TEMPO CNC	42 ± 6	43 ± 7	12 ± 3	3 ± 2
S-TEMPO CNC	51 ± 19	33 ± 13	6 ± 4	10 ± 7
S-CNC	30 ± 7	37 ± 13	13 ± 6	20 ± 7

3.3.2 Conductometric Titrations

Surface charge density of the CNCs was determined using titration. This titration can be viewed in the supplementary information. Within the graph the curve was divided into three parts: HCl titration, CNC surface charge titration and excess NaOH. This information helps calculate one of the surface charge variables needed. The following equation was used to calculate the concentration of negatively charged functional groups:

$$\frac{mmol\ negativly\ charged\ functional\ groups}{kg\ cellulose} = \frac{C_{NaOH} * V_{NaOH}}{W_{CNC}}$$

Where C_{NaOH} is the molar concentration of base used in the titration, V_{NaOH} is the volume used to get the change in curve during the titration, and W_{CNC} is the weight in grams of the CNCs added to the titration.

Sodium chloride was added to the solution because the phase behavior of CNCs is sensitive to electrolytes. By adding an electrolyte, the phase shifts from being predominantly anisotropic to isotropic.[107] An isotropic solution is favorable because the conductivity values are more precise.

Variations in the volume of base added to deprotonate CNCs increased after the synthesis of TEMPO CNC, S-TEMPO CNC, and S-CNC. After normalization, the plain CNCs had little to no surface charge. CNC-1 and CNC2 were prepared through acid hydrolysis. The acid used in this process was sulfuric acid, so a minimal charge was expected. The slurry CNC-2 had a lower concentration of negative charge than the CNC-1.

TEMPO CNC graphs produced a more pronounced U-shape compared to other functionalized CNCs. It is assumed that this is because of the high negative charge density and possibly an effect of the presence of carboxyl groups. By adding salt to the reaction vessel, the severity of the U-shape lessened and made it closer to a V shape. The salt did not only affect the TEMPO CNC samples. It also created a sharper curve for all the samples. Since the TEMPO CNCs surface charge value was so large, the amount of sulfur seen on EDS was minimal. This supports the theory that the groups added were carboxyl groups and not sulfate.

S-CNCs had an enormous increase in charge density, indicating that many of the surface hydroxyl groups on the CNCs were converted to sulfate groups. With S-TEMPO CNC sulfated the same way as S-CNC, it is assumed that the residual secondary hydroxyl groups that were not oxidized would be sulfated along with the other hydroxyl groups that were mobile enough to be reactive. S-TEMPO CNCs charge density increased considerably from the parent TEMPO CNCs. It should be stated that the conductometric titrations measure the amplitude of the charge density of the sample and do not indicate what functional group is producing the result.

Table 2: Conductometric titration data giving charge density of plain CNC and different cellulose nanocrystal functionalization. All functionalized CNCs showed a much larger surface charge than their initial sample. CNC-1 has a sufficient amount more negatively charged groups than that of CNC-2

	Surface Charge (mmol negative charge/kg CNC)
CNC-1	72 ± 32
CNC-2	39 ± 29
TEMPO CNC	500 ± 172
S-TEMPO CNC	566 ± 83
S-CNC	327± 14

3.3.3 Transition Electron Microscopy

Transition electron microscopy (TEM) images were taken to see if the characteristic rod-like crystalline structure of CNCs was maintained after the surface functionalization reactions. Figure 2 shows the morphology was retained through all the synthesis, and the sample

did not degrade into more simple carbohydrates. The aggregation of the particles observed in the image occured during the drying step after the CNCs were stained.[2]

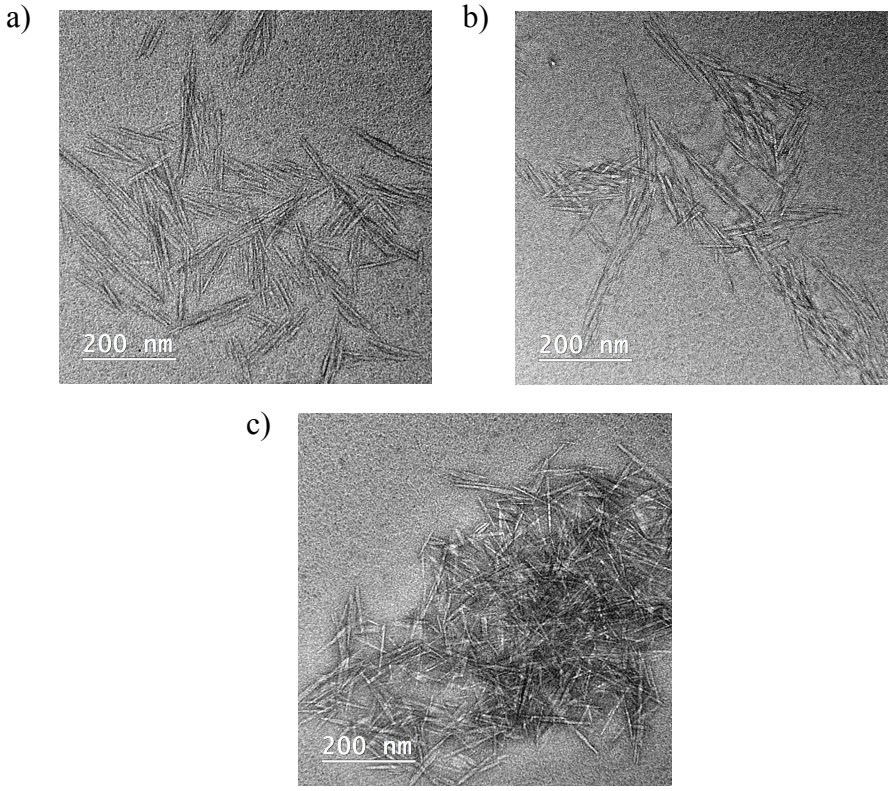

Figure 2: *Transition electron microscopy images of CNCs stained with NanoVan showing the maintained morphology of samples after synthesis a) TEMPO CNC b) S-TEMPO CNC c) S-CNC*

3.3.4 Attenuated Total Reflectance Fourier-Transform Infrared Spectroscopy

The functionalization of CNCs was further characterized through ATR-FTIR. The previous data characterized the qualitative chemistry of the surface and total negative charge but not the specific chemical groups present in the material. Through ATR-FTIR, shown in Figure 3, we were able to demonstrate that sulfate and carboxyl groups replaced the original hydroxyl groups. The stretching peak around 1040 cm^{-1} is due to the C-O-C pyranose ring stretching vibration in cellulose, showing that the CNC ring structure was maintained throughout each process.[150] TEMPO CNC exhibited a peak around 1605 cm^{-1}, which was interpreted to be -COONa.[151] Different studies assign a variety of peaks for certain functional groups, like S=O. One paper suggested the peak for S=O is around 1200 cm^{-1}, whereas another suggested it is at 1240 cm^{-1}.[12, 152] The peak we observed from S-CNC and S-TEMPO CNC was in between the two at 1220 cm^{-1}. The peak detected at 786 cm^{-1} was assigned to the C-O-S bonds created

through sulfation. Therefore, the TEMPO CNC and S-CNC were fully functionalized in the way we predicted. The –COONa peak in S-TEMPO CNC was diminished, showing that the sulfate functionalization reduced the amount of carboxyl groups on the surface and potentially could have replaced them with the sulfate groups. Each sample analyzed of unfunctionalized CNCs did not show any significant difference.

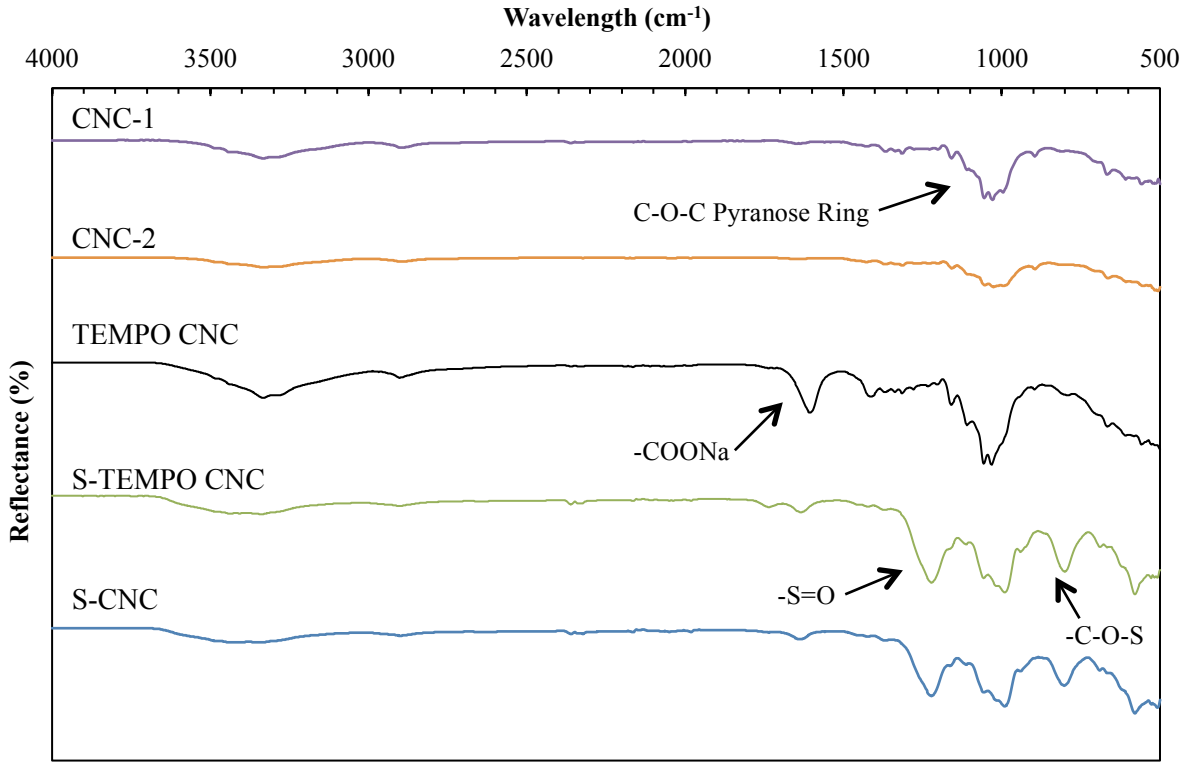

Figure 3: ATR-FTIR spectra of CNC-1, CNC-2, TEMPO CNC, S-TEMPO CNC, and S-CNC. These spectra demonstrate the presence of new functional groups in TEMPO CNC, S-TEMPO CNC, and S-CNC signifying that the synthesis conducted was effective at altering the surface hydroxyl groups.

3.3.5 Clotting Assays

Activated thromboplastin time (aPTT) is a measure of the intrinsic pathway which include factors I, II, V, VIII, IX, X, XI, and XII. Normal clotting time values ranged from 25-37 seconds, with our control being within that range at 28.8 seconds. Two samples, S-CNC and S-TEMPO CNC, gave results similar to other heparin mimics made from sulfated and carboxylated chitosan and a carbohydrate backbone. The sulfated CNC samples had values >300 seconds at 500 µg/mL and were able to maintain a high clotting time at 50 µg/mL (see Figure 4). Published values of heparin aPTT tests show that, to observe a 200 second clotting time, 13.8 µg/mL of heparin

needs to be added to the system and 5.6 μg/mL for a 100 second clotting time.[153] For S-CNC to have a 200 second clotting time the concentration of CNCs presented on the exterior of the material must reach is 50 μg/mL, which is significantly higher than that of heparin. Since our end goal is to create a material, the limiting factor is the ability to incorporate functionalized CNCs into the composite. With the anti-clotting ability reaching long clotting times around 50 μg/mL the composite CNC concentration just needs to reach this concentration to limit clotting. The material will not release the incorportated CNCs into the system because the CNCs are held together by the polymer base. The CNCs will also not be metabolized due to heparinase not recognizing the sequence. This idea and the mechanism that would produce the results needs to be tested and further looked into with the functionalized CNCs produced in this work. Over the long term, the amount of CNCs used will be less than that of heparin because its anticoagulation properties are not time dependent.

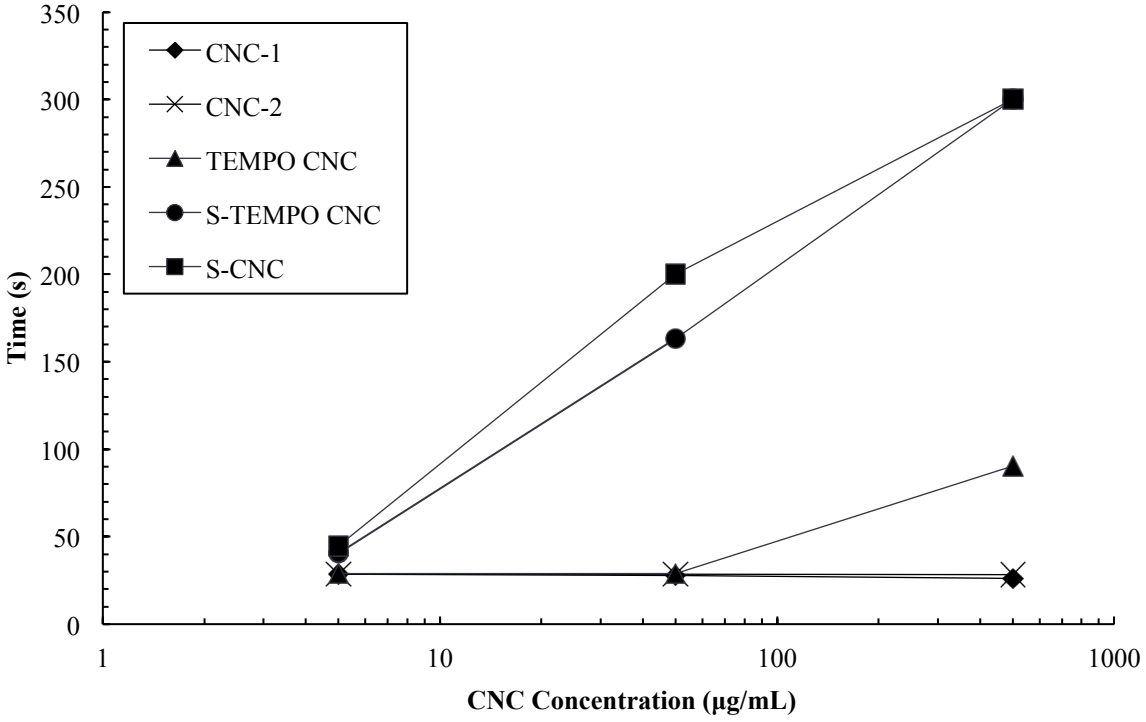

Figure 4: aPTT assay of plain and derivatized CNC samples with the concentrations starting at 500 μg/mL and going down by 1:10 serial dilutions. Once the clotting time reached 300 seconds the experiment was ended assuming the sample would not clot. The S-CNCs and S-TEMPO CNCs gave the best anticoagulation activity showing they have the ability to inhibit the intrinsic clotting pathway.

Prothrombin time (PT) examines clotting initialized through the extrinsic pathway. This pathway is initiated by external trauma that causes blood to escape from the vascular system. Blood factors analyzed in PT assays are factors I, II, V, VII, and X.[83] Often, this test is carried out to check for the blood clotting rate in patients taking warfarin, because vitamin K is needed to make the active clotting factors. Standard values were measured by adding only plasma and buffer to give an uninhibited 12 second clotting time. The results of this assay (seen in Table 3) demonstrate that S-CNC provides the best anti-clotting results, followed by S-TEMPO CNC. Heparin works by inhibiting clotting factors in the intrinsic pathway, so the ability of our material to limit the extrinsic pathway as well is promising for anticoagulation. This test also indicates that sulfur substitutions are more effective than carboxyl substitutions at inhibiting the extrinsic pathway.

Table 3: Average PT assay of differently functionalized cellulose nanocrystals with the clotting measured in seconds and rounded to the nearest 0.5. Samples with the largest concentration of sulfate groups, S-TEMPO CNC and S-CNC demonstrated the ability to inhibit the extrinsic pathway to up to 500 µg/mL and 50 µg/mL for S-CNC. Samples with lower concentrations of sulfate groups and high concentrations of carboxyl groups were not able to reduce coagulation

	Clotting of CNCs (sec)			
	0.5 µg/mL	**5 µg/mL**	**50 µg/mL**	**500 µg/mL**
CNC-1	19.0	19.5	19.0	17.0
CNC-2	18.5	18.0	18.0	16.5
TEMPO CNC	15.5	15.0	15.0	15.0
S-TEMPO CNC	19.5	17.5	29.0	>75
S-CNC	14.0	15.0	>75	>75

Thrombin time (TT) is a highly sensitive and not very descriptive test that measures the conversion of fibrinogen to fibrin through the addition of bovine thrombin. This conversion step is one of the last in the coagulation cascade in the common pathway. The factors that are specifically inhibited are unknown when using this test because of its position in the pathway. It does show the ability/inability for a sample to form a clot because fibrin is the mesh necessary for the stabilization of a platelet plug.

Abnormal fibrinogen production and heparin use are the two main factors that prolong the TT assay results.[84] We were able to rule out abnormal fibrinogen production by conducting a

control with plasma and thrombin, which gave a clotting time of 17.5 seconds. Other tests measuring heparin's impact on clotting, like aPTT assays, are more commonly used than the TT assay. Results of this assay, shown in table 4, show that S-CNC, followed by S-TEMPO CNC, then CNC-1 inhibit coagulation the most. The S-CNCs showed excellent results because the concentration at which it induced coagulation was at 0.05 μg/mL. Compared to the results reported in other papers, this is an order of magnitude lower concentration or better than other heparin mimics at limiting coagulation.[63] With sulfur concentration on the plain CNCs being CNC-2 < CNC-1 and the TT assays mirroring this effect in clotting time, the sulfur concentration is thought to have a large impact on anticoagulation. This theory is especially presented in the TT assay results where CNC-1 produces similar or better anti-clotting properties than the TEMPO CNC and S-TEMPO.

The ability of TEMPO CNC to inhibit coagulation shows that either negative charge density has a part in anticoagulation, or carboxyl groups are able to limit anticoagulation. From the results of CNC-1 and S-TEMPO CNC, it is presumed that the presence of sulfur groups and charge density, not carboxyl groups, are the factors affecting coagulation.

Table 4: Average TT assay of differently functionalized cellulose nanocrystals with the clotting measured in seconds and rounded to the nearest 0.5. Sample S-CNC showed the greatest anticoagulation capacity, with S-TEMPO CNC next, then CNC-1. TEMPO CNC, although having the highest negative charge density, could not limit coagulation as much as S-CNC. This suggests that clotting abilities in the intrinsic pathway are highly interconnected to sulfate concentration.

	Clotting of CNCs (sec)				
	0.05 μg/mL	**0.5 μg/mL**	**5 μg/mL**	**50 μg/mL**	**500 μg/mL**
CNC-1	--	14.0	>75	>75	>75
CNC-2	--	14.0	14.5	>75	>75
TEMPO CNC	--	12.5	13.8	15.5	>75
S-TEMPO CNC	--	13.5	>75	>75	>75
S-CNC	12.5	>75	>75	>75	>75

3.3.6 Platelet Adhesion

Platelets were found to adhere on all CNC samples as seen in Figure 5. The TEMPO CNC samples showed the least platelet adhesion. Platelets were not observed on the control

group of samples treated using platelet poor plasma. Platelets adhered the most to surfaces with rough topography. The smoother topography areas on the samples showed much less platelet adherence and fewer spread dendritic platelets. Using terminology from Grunkemeier, the platelets that adhered to the PU and TEMPO CNC sample were round with no pseudopodia present.[154] Whereas, CNC-1, S-TEMPO CNC, and S-CNC showed dendritic and spread dendritic platelets. CNC-1 and S-CNC showed some platelets that had spread, but the S-TEMPO CNCs did not.

This data shows that, although sulfate groups are able to inhibit anticoagulation, carboxyl groups have the ability to limit platelet adhesion the most. Flat surfaces also had an impact on the attachment of platelets. Smoother more hydrophilic surfaces result in fewer platelets compared to rough surfaces. Samples created through solvent casting resulted in highly topographical surfaces. Surfaces with the most topography showed the most platelet adhesion. To limit this future studies should look into melt pressing the samples before conducting the fixing assay. The combination of carboxyl groups needed to inhibit platelet fixing will need to be further investigated to find the desired sulfate and carboxyl concentration for ideal anticoagulation and inhibition of platelet adhesion.

Polyurethane is a polymer known to stimulate platelet adhesion. However, compared to other materials it does have good hemocompatibility.[6] With this knowledge and using PU as a control, we were able to investigate if our material surface increased or decreased platelet adhesion.

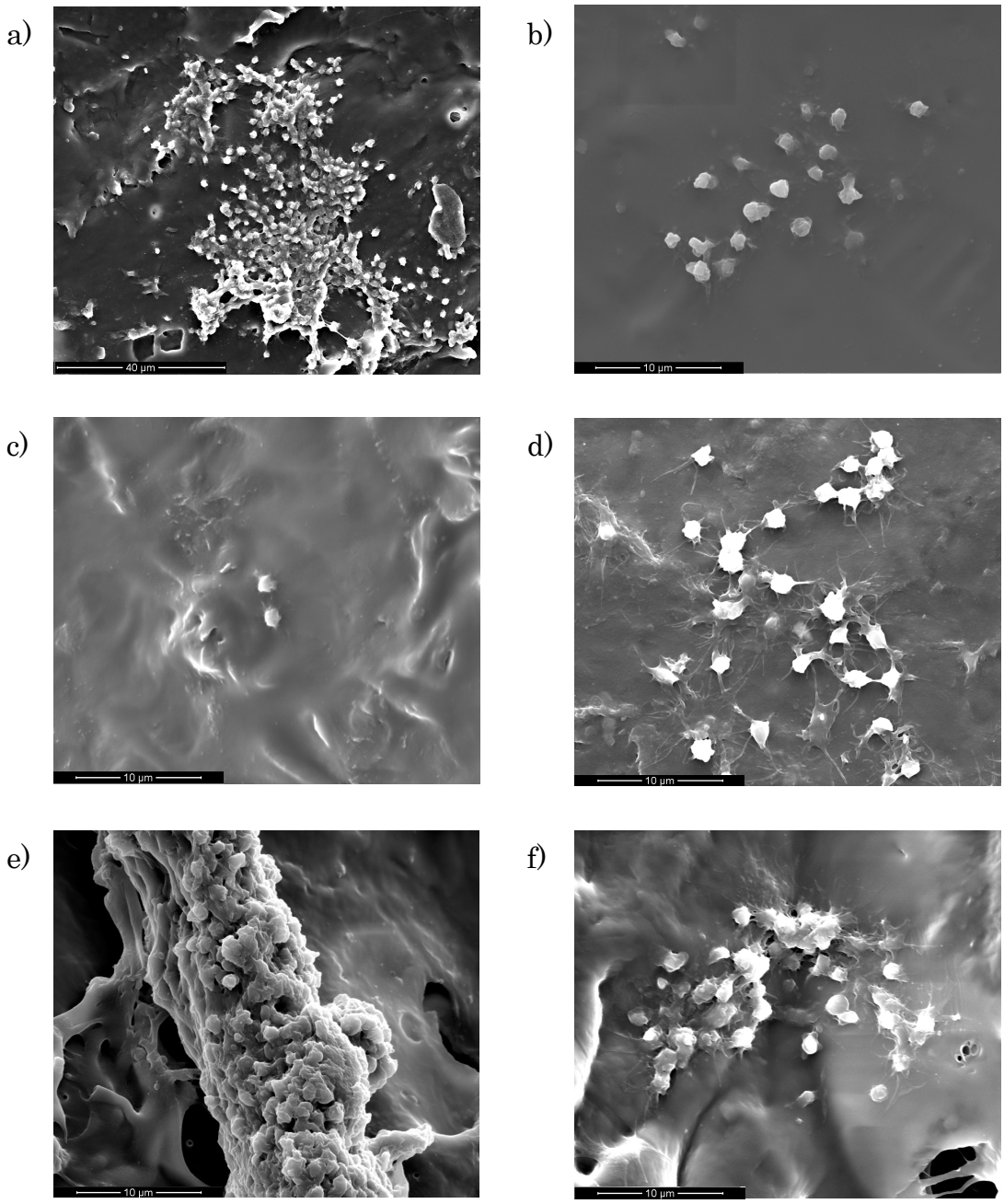

Figure 5: Scanning electron microscope images of platelets grown on CNC surfaces through platelet rich plasma with a) 2500x magnification S-CNC and 7500x magnification b) polyurethane control sample c) CNC-1 d) TEMPO CNC e) S-TEMPO CNC f) S-CNC. TEMPO CNCs showed the least platelet growth along and adherence to the sample. Highly topographical samples, like the S-TEMPO CNC, sample produces large platelet activity.

3.4 Conclusion

Cellulose nanocrystals functionalization with carboxyl and sulfate groups has been characterized by EDS, ATR-FTIR, and conductometric titration. After these different synthesis

methods we determined through TEM imaging that none of the samples lost their characteristic rod-like morphology. By keeping the structure, when added to a composite the CNCs will still maintain their mechanical benefits as well as producing anticoagulation properties. Of the samples synthesized, the sulfated CNCs and sulfated TEMPO CNCs showed the best anticoagulation properties. This was demonstrated in aPTT and TT assays. The sulfated CNCs proved superior to other materials examined in the past, needing an order of magnitude less concentration than other heparin mimics. A sulfated amine similar to the functional group on the ATBR was synthesized, but the results yielded inconclusive functionalization.

The blood clotting results obtained using CNCs indicates that the sulfate concentration is the determining factor for inhibiting coagulation when using long chain crystalline cellulose. The net negative charge density on the CNCs for anticoagulation to occur was not the limiting factor. This was shown by the carboxyl groups being unable to inhibit coagulation even at a higher concentration than sulfate groups. The plain CNC samples, CNC-1 and CNC-2, showed this best in the TT assays. Both samples were able to limit coagulation better than the TEMPO CNCs, even though their sulfate concentration was very minimal. This is in contrast with the results of Li who showed that a 2:3 and 3:2 wt % ratio of carboxyl to sulfate groups give the best anticoagulation results, even compared with full sulfonation, with the higher sulfate wt% being slightly better.[144]

Platelet aggregation was reduced the greatest on TEMPO CNC samples. Since platelet adherence is not directly inhibited by heparin it is not surprising that sulfate concentration is not the limiting factor. A hemocompatible polymer should also be examined knowing that the samples do not limit platelet adherence enough to quantitate platelet adhesion. This may lead to interpretable results if the polyurethane, surface of the sample, or the CNCs themselves are influencing platelet adherence. In conclusion we have demonstrated that functionalized cellulose nanocrystals can be utilized to create a biomedical composite material that can replace heparin in some situations.

4 Conclusion

Altering the functional groups of CNCs from hydroxyl groups to carboxyl and/or sulfate groups changed the surface chemistry but not the morphology. Through TEM imaging the samples showed that even after all the synthesis conducted they still maintained their rod-like

structure. This ensures that the addition of the CNCs to a polymer composite will help promote higher strength properties.

Cellulose nanocrystals (CNCs) that underwent sulfation and TEMPO oxidation showed improvement in their anticoagulation properties. These were shown in aPTT, TT, and PT assays. All assays exhibited S-CNC reduced coagulation the greatest with S-TEMPO CNC following. Observing the two unmodified CNCs that had different surface sulfation concentrations from acid hydrolysis along with comparing these samples to TEMPO CNCs produced presented sufficient information that the functional group that limits coagulation the most when comparing two groups that are present on the antithrombin binding region, sulfate and carboxyl groups, sulfate is the most important.

The two unmodified CNCs, CNC-1 and CNC-2, contained different sulfate charge densities with CNC-1 being almost double that of CNC-2. The negative charge density, while larger than CNC-2, is still 4.5 times lower than S-CNCs concentration. The minimal charge density difference in the grand scheme of all samples showed increases in anticoagulation in TT and PT assays with CNC-1 outperforming CNC-2. This result helps prove that sulfate concentration is the main functional group that is important in anticoagulation. Another result from the data that backed up this theory is the coagulation of TEMPO oxidized samples compared to the unmodified sulfate charged samples. TEMPO CNC samples with over 200 mmol/kg higher negative charge density compared to sulfate groups to CNC-1 showed better anticoagulation in the TT assay and similar results in the PT assay.

Characterization of the differently functionalized CNCs through EDS, conductometric titration, and ATR-FTIR proved the functionalization change from hydroxyl groups to carboxyl or sulfate. EDS characterization gave qualitative evidence that after sample synthesis sulfur elements were added to the S-CNC sample and S-TEMPO CNC sample. CNC-1, CNC-2, and TEMPO CNC showed minimal evidence of sulfur after standard deviation was taken into consideration. Comparing CNC-1 to CNC-2 using EDS shows that CNC-1 contains a minimal amount more sulfur elements in the bulk of the sample.

Conductometric titration produced quantitative values for charged groups that were synthesized on the surface of the CNCs. Surface charge density was measured through the calculation of the amount of NaOH base it takes to remove all the protons on the samples surface. Curves obtained from CNC-1 and CNC-2 gave more V-like curves, showing a lower charge

density. Titrations done using TEMPO CNC gave curves more resembling a U, showing a higher charge density. These titrations exhibited that charge density varied with the highest to lowest being S-TEMPO CNC, TEMPO CNC, S-CNC, CNC-1, and CNC-2. TEMPO CNC samples run were from 3 different batches made at three different times. This is why the standard deviation for this sample is so high compared to the others. Each other sample only contains data from one batch prepared.

ATR-FTIR data helped combined both the EDS and conductometric titrations to produce sufficient evidence needed to show the CNC samples had been correctly functionalized to the hypothesized functional groups. Data also displayed that the cyclohexane rings were maintained even after all the synthesis had been completed. The lack of –S=O and –C-O-S peaks in CNC-1 and CNC-2 were most likely a result of the concentration of these functional groups being so minimal in the sample. Synthesis of the samples was not homogeneous throughout, shown in standard deviation of conductometric titration samples, so the S-TEMPO CNC sample lacking the –COO peak is most likely due to this. Another sample would have been run but the data was analyzed after creating solutions for platelet fixing and no more sample was left. The clotting results combined with the characterization does back up the fact that the sample is some form of a combination of sulfate and carboxyl groups. Lower clotting values with higher charge density with only sulfate groups would not make sense with the other data provided, while partial groups with lower clotting values does.

Platelet fixing done on the surface of the 30:70 wt % CNC:PU composites showed stimulated platelet adherence. Samples that showed the least platelet growth were TEMPO CNC/PU composites. This agrees with previous work done stating that carboxyl groups limited protein adhesion onto surfaces better than other functional groups. Protein adhesion leads to platelet adherence so these two effects go hand in hand. Five PRP and PPP samples were analyzed with them all showing similar results to each sample. Samples with rougher surfaces stimulated more platelets adhesion, whereas smoother samples had fewer platelets.

5 Future Work

This project has created the basis for identifying an effective, non-animal based CNC composite material that inhibits coagulation. The next steps that should be taken should involve incorporating S-CNC, the most promising of the samples, into several polymer composites. Three methods of CNC addition to a composite should be attempted. The first should have the

CNCs sonicated into solution then added to the material, the second the CNCs should be dusted on the outside while the material is curing, and the third should combine the two methods.

These samples should then undergo tests showing blood flow through the material for 4-8 hours looking for platelet adhesion. Hemodialysis (HD) treatments only consist of 4-6 hour treatments so this time frame plus two hours additional time should define the initial testing. It would provide a realistic estimate of the workability of the material even in extreme clinical situations. If coagulation can be inhibited for this long then the test should be extended to determine the limits. Depending on the results, the CNC composites could be tested for expansion of uses from an additive in HD to use in biomedical materials such as catheters or artificial organs.

Before testing, the composites should be melt pressed to reduce the contribution of surface roughness on platelet adhesion to the material. Initial tests should use a high concentration of S-CNC to make sure if the material can inhibit clotting it would be observed. After, if coagulation is inhibited to a high enough degree, the concentration of CNCs could be lowered systematically to find the minimum amount needed for coagulation to be limited.

If possible, micro-etching the surface of the CNC or chitosan composite material material should be considered so its topography mimics that of blood vessels. This topography would be revealed using techniques such as atomic force microscopy (AFM). Past work that mimicked sharkskin was able to reduce marine biofouling similar to how sharkskin naturally does. In the same way, mimicking blood vessel topography could possibly also reduce coagulation. Topography changes in the material can potentially create a superhydrophilic material, so contact angle tests should be carried out to show the differences that concentration, topography, using chitin over cellulose, and type of reinforcement polymer can have on contact angle and coagulation.

Along with blood tests, biocompatibility tests should also be done looking at leeching of CNCs or polymer from the matrix, biofouling, biocompatibility, cell cultures, *in vitro* and *in vivo* testing, and CNCs interaction in blood. CNCs are considered biocompatible, but additional studies should be carried out to determine the impact of CNCs added into the blood on the body's response. This is important to consider in case the polymer leeches out or releases CNCs into the system. Even if they do not create a side effect, it will be important to determine the ability of the body to metabolize the product. Since the CNCs are functionalized to inhibit

coagulation, it is important to know this in case the body cannot metabolize CNCs and they stay in the system continuously reducing clotting. CNCs in the body could potentially initiate cell signaling pathways, upregulation of enzymes, or other biological processes that could harm the individual. This would need to be studied through in vitro and in vivo testing, including several locations in the body that would be susceptible to interaction with products of this material such as the heart and blood vessels. All these different interactions have the potential to pose major threats to patient's well being. This is particularly true for HD patients, who undergo continuous treatments.

Mechanical testing of the material must also be conducted to see if it has the strength and stiffness needed. Since dialysis is administered using negative pressure, the material needs to be stiff enough to not collapse from the absence of pressure, which would reduce blood flow. The material also undergoes pressing from the peristaltic pump which helps move blood through the EC. The material will need to be strong enough to withstand repeated flexion and compression from the rollers in the pump. CNCs within the material would also need to be able to withstand these movements and not flake off the surface and enter the bloodstream. The ability to resist kinking is important because the tubing is sometimes long and can get caught on something and kink. This kinking, similar to the problem of collapsing, would reduce blood flow during the procedure. The glass transition of the final material should be measured because adding sulfate groups has shown to lower the degradation temperature of the sample. Though HD materials should not experience heat much over room temperature levels or below freezing, it is important to know this transition temperature for possible future circumstances the material could be in, for example the heat or cold in a shipping container or delivery truck.

To enter the U.S. market, the FDA approval process must be completed. The composite being created would most likely be a class II material that needs 510(k) approval. Since it is just an alteration of the currently used dialysis tubing, it should be able to skip premarket application (PMA). This must be carefully examined though because CNC products may need to be present in the market to use the 510(k) process. After completing the 510(k) submission the ability to produce the highest quality but fastest produced product will need to be researched. This research would include finding the ideal surface charge of S-CNCs, the time and mole concentration for the sulfonation reaction to get this charge, and the scaling of this process.

Recent research trends show the investigation of using chitosan as an anticoagulant is rising. Chitosan is a popular polymer being used because it is highly abundant and has an amine group natuarally present on the surface. This amine can be functionalized to add a sulfate creating molecule that has high affinity to AT. Most of the testing done on sulfated chitosan has focused on measuring the ability of the chitosan's anticoagulant properties, applications as a hydrogel, or the effect of different factors on anticoagulation. Very little testing has been done on composite materials made with chitosan and their anticoagulant effects. Most material testing of chitosan has been of hydrogels. Future work should explore the use of using chitosan nanocrystals, similar to our work with cellulose nanocrystals, as a material reinforcement and anticoagulant. Though sulfonation of chitosan has shown to be more hazardous than that of CNCs, the anticoagulation results present higher anticoagulation at lower concentrations. Having less additive in a polymer material would make it easier to create a homogenous material, while still having the desired clotting properties.

References

1. Postek, M. T.; Vladar, A.; Dagata, J.; Farkas, N.; Ming, B.; Wagner, R.; Raman, A.; Moon, R. J.; Sabo, R.; Wegner, T. H.; Beecher, J., Development of the metrology and imaging of cellulose nanocrystals. *Meas. Sci. Technol.* **2011,** *22* (2), 10.

2. Habibi, Y.; Lucia, L. A.; Rojas, O. J., Cellulose Nanocrystals: Chemistry, Self-Assembly, and Applications. *Chem. Rev.* **2010,** *110* (6), 3479-3500.

3. Ng, H.-M.; Sin, L. T.; Tee, T.-T.; Bee, S.-T.; Hui, D.; Low, C.-Y.; Rahmat, A. R., Extraction of cellulose nanocrystals from plant sources for application as reinforcing agent in polymers. *Composites Part B: Engineering* **2015,** *75*, 176-200.

4. Moon, R. J.; Martini, A.; Nairn, J.; Simonsen, J.; Youngblood, J., Cellulose nanomaterials review: structure, properties and nanocomposites. *Chem. Soc. Rev.* **2011,** *40* (7), 3941-3994.

5. Riddel Jr, J. P.; Aouizerat, B. E.; Miaskowski, C.; Lillicrap, D. P., Theories of blood coagulation. *Journal of pediatric oncology nursing* **2007,** *24* (3), 123-131.

6. Xu, L.-C.; Bauer, J.; Siedlecki, C. A.; Group, A. C. f. t. H. a. B. I. R., Proteins, Platelets, and Blood Coagulation at Biomaterial Interfaces. *Colloids and surfaces. B, Biointerfaces* **2014,** *124*, 49-68.

7. Fu, L.; Suflita, M.; Linhardt, R. J., Bioengineered heparins and heparan sulfates. *Advanced Drug Delivery Reviews* **2016,** *97*, 237-249.

8. Tovar, A. M. F.; Teixeira, L. A. C.; Rembold, S. M.; Leite, M.; Lugon, J. R.; Mourão, P. A. S., Bovine and porcine heparins: different drugs with similar effects on human haemodialysis. *BMC Research Notes* **2013,** *6* (1), 230.

9. Paluck, S. J.; Nguyen, T. H.; Maynard, H. D., Heparin-Mimicking Polymers: Synthesis and Biological Applications. *Biomacromolecules* **2016,** *17* (11), 3417-3440.

10. Liu, X. Y.; St Ange, K.; Fareed, J.; Hoppensteadt, D.; Jeske, W.; Kouta, A.; Chi, L. L.; Jin, C. J.; Jin, Y. S.; Yao, Y. M.; Linhardt, R. J., Comparison of Low-Molecular-Weight Heparins Prepared From Bovine Heparins With Enoxaparin. *Clin. Appl. Thromb.-Hemost.* **2017,** *23* (6), 542-553.

11. Onishi, A.; St Ange, K.; Dordick, J. S.; Linhardt, R. J., Heparin and anticoagulation. *Front. Biosci.* **2016,** *21*, 1372-1392.

12. Wang, Z. M.; Xiao, K. J.; Li, L.; Wu, J. Y., Molecular weight-dependent anticoagulation activity of sulfated cellulose derivatives. *Cellulose* **2010,** *17* (5), 953-961.

13. Yates, E. A.; Rudd, T. R., Recent innovations in the structural analysis of heparin. *Int. J. Cardiol.* **2016,** *212*, S5-S9.

14. Wannamaker, E.; Kondo, K.; Johnson, D. T., Heparin-Induced Thrombocytopenia and Thrombosis: Preventing your Thrombolysis Practice from Taking a HITT. *Seminars in Interventional Radiology* **2017,** *34* (4), 409-414.

15. Casu, B.; Naggi, A.; Torri, G., Re-visiting the structure of heparin. *Carbohydrate Research* **2015,** *403*, 60-68.

16. Huang, Y. S.; Taylor, L.; Chen, X. P.; Ayres, N., Synthesis of a Polyurea from a Glucose- or Mannose-Containing N-Alkyl Urea Peptoid Oligomer. *J. Polym. Sci. Pol. Chem.* **2013,** *51* (24), 5230-5238.

17. Huang, Y.; Shaw, M. A.; Warmin, M. R.; Mullins, E. S.; Ayres, N., Blood compatibility of heparin-inspired, lactose containing, polyureas depends on the chemistry of the polymer backbone. *Polym. Chem.* **2016,** *7* (23), 3897-3905.

18. Fu, L.; Li, G. Y.; Yang, B.; Onishi, A.; Li, L. Y.; Sun, P. L.; Zhang, F. M.; Linhardt, R. J., Structural characterization of pharmaceutical heparins prepared from different animal tissues. *J. Pharm. Sci.* **2013,** *102* (5), 1447-1457.

19. Peysselon, F.; Ricard-Blum, S., Heparin–protein interactions: From affinity and kinetics to biological roles. Application to an interaction network regulating angiogenesis. *Matrix Biology* **2014,** *35* (Supplement C), 73-81.

20. Hayman, E. G.; Patel, A. P.; James, R. F.; Simard, J. M., Heparin and Heparin-Derivatives in Post-Subarachnoid Hemorrhage Brain Injury: A Multimodal Therapy for a Multimodal Disease. *Molecules* **2017,** *22* (5), 18.

21. Cassinelli, G.; Naggi, A., Old and new applications of non-anticoagulant heparin. *Int. J. Cardiol.* **2016,** *212*, S14-S21.

22. Jeffrey D. Esko, J. H. P., and Robert J. Linhardt., Proteins That Bind Sulfated Glycosaminoglycans. In *Essentials of Glycobiology*, Cold Spring Harbor Laboratory Press: Cold Spring Harbor (NY), 2015-2017; Vol. 3.

23. Capila, I.; Linhardt, R. J., Heparin - Protein interactions. *Angew. Chem.-Int. Edit.* **2002,** *41* (3), 391-412.

24. Hasan, M.; Najjam, S.; Gordon, M. Y.; Gibbs, R. V.; Rider, C. C., IL-12 is a heparin-binding cytokine. *J. Immunol.* **1999,** *162* (2), 1064-1070.

25. Najjam, S.; Gibbs, R. V.; Gordon, M. Y.; Rider, C. C., Characterization of human recombinant interleukin 2 binding to heparin and heparan sulfate using an ELISA approach. *Cytokine* **1997,** *9* (12), 1013-1022.

26. Liu, H. Y.; Zhang, Z. Q.; Linhardt, R. J., Lessons learned from the contamination of heparin. *Nat. Prod. Rep.* **2009,** *26* (3), 313-321.

27. Hirsh, J.; Bauer, K. A.; Donati, M. B.; Gould, M.; Samama, M. M.; Weitz, J. I., Parenteral Anticoagulants. *CHEST 133* (6), 141S-159S.

28. Torri, G.; Naggi, A., Heparin centenary - an ever-young life-saving drug. *Int. J. Cardiol.* **2016,** *212*, S1-S4.

29. Casu, B.; Naggi, A.; Torri, G., Re-visiting the structure of heparin. *Carbohydrate Research* **2015,** *403* (Supplement C), 60-68.

30. Olson, S. T.; Chuang, Y. J., Heparin activates antithrombin anticoagulant function by generating new interaction sites (exosites) for blood clotting proteinases. *Trends Cardiovasc. Med.* **2002,** *12* (8), 331-338.

31. Schoen, P.; Wielders, S.; Petitou, M.; Lindhout, T., The effect of sulfation on the anticoagulant and antithrombin III-binding properties of a heparin fraction with low affinity for antithrombin III. *Thromb. Res.* **1990,** *57* (3), 415-423.

32. Fromm, J. R.; Hileman, R. E.; Caldwell, E. E. O.; Weiler, J. M.; Linhardt, R. J., Differences in the Interaction of Heparin with Arginine and Lysine and the Importance of these Basic Amino Acids in the Binding of Heparin to Acidic Fibroblast Growth Factor. *Archives of Biochemistry and Biophysics* **1995,** *323* (2), 279-287.

33. Jin, J.-f.; Zhu, L.-l.; Chen, M.; Xu, H.-m.; Wang, H.-f.; Feng, X.-q.; Zhu, X.-p.; Zhou, Q., The optimal choice of medication administration route regarding intravenous, intramuscular, and subcutaneous injection. *Patient preference and adherence* **2015,** *9*, 923.

34. Guan, Y. D.; Xu, X. H.; Liu, X. Y.; Sheng, A. R.; Jin, L.; Linhardt, R. J.; Chi, L. L., Comparison of Low-Molecular-Weight Heparins Prepared From Bovine Lung Heparin and Porcine Intestine Heparin. *J. Pharm. Sci.* **2016,** *105* (6), 1843-1850.

35. Liu, Z.; Ji, S.; Sheng, J.; Wang, F., Pharmacological effects and clinical applications of ultra low molecular weight heparins. *Drug Discoveries & Therapeutics* **2014,** *8* (1), 1-10.

36. Walenga, J. M.; Lyman, G. H., Evolution of heparin anticoagulants to ultra-low-molecular-weight heparins: A review of pharmacologic and clinical differences and applications in patients with cancer. *Critical Reviews in Oncology/Hematology* **2013,** *88* (1), 1-18.

37. Zulueta, M. M. L.; Lin, S.-Y.; Hu, Y.-P.; Hung, S.-C., Synthetic heparin and heparan sulfate oligosaccharides and their protein interactions. *Current Opinion in Chemical Biology* **2013,** *17* (6), 1023-1029.

38. van der Meer, J. Y.; Kellenbach, E.; van den Bos, L. J., From Farm to Pharma: An Overview of Industrial Heparin Manufacturing Methods. *Molecules* **2017,** *22* (6), 13.

39. Conners, M. S.; Money, S. R., The New Heparins. *The Ochsner Journal* **2002,** *4* (1), 41-47.

40. Weitz, J. I., Low-molecular-weight heparins (vol 337, pg 688, 1997). *N. Engl. J. Med.* **1997,** *337* (21), 1567-1567.

41. Hirsh, J.; Warkentin, T. E.; Shaughnessy, S. G.; Anand, S. S.; Halperin, J. L.; Raschke, R.; Granger, C.; Ohman, E. M.; Dalen, J. E., Heparin and Low-Molecular-Weight Heparin Mechanisms of Action, Pharmacokinetics, Dosing, Monitoring, Efficacy, and Safety. *CHEST* **2001,** *119* (1), 64S-94S.

42. Steigerwalt, R. D.; Pascarella, A.; De Angelis, M.; Ciucci, F.; Gaudenzi, F., An ultra-low-molecular-weight heparin, fondaparinux, to treat retinal vein occlusion. *Drug Discov. Ther.* **2016,** *10* (3), 167-171.

43. Linhardt, R. J.; Liu, J., Synthetic heparin. *Curr. Opin. Pharmacol.* **2012,** *12* (2), 217-219.

44. Heparin for Drug and Medical Device Use: Monitoring Crude Heparin for Quality. FDA: 2013.

45. Keire, D., Safeguarding the global heparin supply chain: Bovine Heparin Initiative. Administration, U. S. F. a. D., Ed. 2016.

46. Vreeburg, J. W.; Baauw, A., Method for preparation of heparin from mucosa. Google Patents: 2010.

47. Manson, L.; Weitz, J. I.; Podor, T. J.; Hirsh, J.; Young, E., The variable anticoagulant response to unfractionated heparin in vivo reflects binding to plasma proteins rather than clearance. *J. Lab. Clin. Med.* **1997,** *130* (6), 649-655.

48. Kalathottukaren, M. T.; Abbina, S.; Yu, K.; Shenoi, R.; Creagh, A. L.; Haynes, C.; Kizhakkedathu, J. N., A Polymer Therapeutic Having Universal Heparin Reversal Activity: Molecular Design and Functional Mechanism. *Biomacromolecules* **2017,** *18* (10), 3343-3358.

49. McKay, D. J.; Renaux, B. S.; Dixon, G. H., The amino acid sequence of human sperm protamine P1. *Bioscience reports* **1985,** *5* (5), 383-391.

50. Cormack, J. G.; Levy, J. H., Adverse Reactions to Protamine. *Coronary Artery Dis.* **1993,** *4* (5), 420-425.

51. Carr, J. A.; Silverman, N., The heparin-protamine interaction - A review. *J. Cardiovasc. Surg.* **1999,** *40* (5), 659-666.

52. Muralidharan-Chari, V.; Kim, J.; Mousa, S. A., Reversal of anticoagulant activity of heparin and low molecular weight heparins by poly-L-lysine: A comparative 'in vitro' study versus protamine sulfate. *Thromb. Res.* **2017,** *155*, 128-130.

53. Wright, A. T.; Zhong, Z. L.; Anslyn, E. V., A functional assay for heparin in serum using a designed synthetic receptor. *Angew. Chem.-Int. Edit.* **2005,** *44* (35), 5679-5682.

54. Ltd, W. U. *Prosulf 10mg/ml Solution for Injection*; electronic Medicines Compendium, 2016.

55. Rabenstein, D. L., Heparin and heparan sulfate: structure and function. *Nat. Prod. Rep.* **2002,** *19* (3), 312-331.

56. Knelson, E. H.; Nee, J. C.; Blobe, G. C., Heparan sulfate signaling in cancer. *Trends in Biochemical Sciences* **2014,** *39* (6), 277-288.

57. Liu, J.; Pedersen, L. C., Anticoagulant Heparan Sulfate: Structural Specificity and Biosynthesis. *Applied microbiology and biotechnology* **2007,** *74* (2), 263-272.

58. Ingle, R. G.; Agarwal, A. S., A world of low molecular weight heparins (LMWHs) enoxaparin as a promising moiety—A review. *Carbohydr. Polym.* **2014,** *106* (Supplement C), 148-153.

59. Kakkar, A. K., Low- and ultra-low-molecular-weight heparins. *Best Pract. Res. Clin. Haematol.* **2004,** *17* (1), 77-87.

60. Cook, B. W., Anticoagulation Management. *Seminars in Interventional Radiology* **2010,** *27* (4), 360-367.

61. Weitz, J. I., Low-Molecular-Weight Heparins. *N. Engl. J. Med.* **1997,** *337* (10), 688-699.

62. Crowther, M. A.; Berry, L. R.; Monagle, P. T.; Chan, A. K. C., Mechanisms responsible for the failure of protamine to inactivate low-molecular-weight heparin. *Br. J. Haematol.* **2002,** *116* (1), 178-186.

63. Huang, Y. S.; Shaw, M. A.; Mullins, E. S.; Kirley, T. L.; Ayres, N., Synthesis and Anticoagulant Activity of Polyureas Containing Sulfated Carbohydrates. *Biomacromolecules* **2014,** *15* (12), 4455-4466.

64. GlaxoSmithKline, ARIXTRA® (fondaparinux sodium) Injection FDA, Ed. 2005.

65. Okamoto, Y.; Yano, R.; Miyatake, K.; Tomohiro, I.; Shigemasa, Y.; Minami, S., Effects of chitin and chitosan on blood coagulation. *Carbohydr. Polym.* **2003,** *53* (3), 337-342.

66. Yang, J. H.; Luo, K.; Li, D. L.; Yu, S. S.; Cai, J.; Chen, L. Y.; Du, Y. M., Preparation, characterization and in vitro anticoagulant activity of highly sulfated chitosan. *Int. J. Biol. Macromol.* **2013,** *52*, 25-31.

67. Suwan, J.; Zhang, Z.; Li, B.; Vongchan, P.; Meepowpan, P.; Zhang, F.; Mousa, S. A.; Mousa, S.; Premanode, B.; Kongtawelert, P.; Linhardt, R. J., Sulfonation of papain treated chitosan and its mechanism for anticoagulant activity. *Carbohydrate research* **2009,** *344* (10), 1190-1196.

68. Maruyama, T.; Toida, T.; Imanari, T.; Yu, G.; Linhardt, R. J., Conformational changes and anticoagulant activity of chondroitin sulfate following its O-sulfonation1. *Carbohydrate Research* **1998,** *306* (1-2), 35-43.

69. Guerrini, M.; Beccati, D.; Shriver, Z.; Naggi, A.; Viswanathan, K.; Bisio, A.; Capila, I.; Lansing, J. C.; Guglieri, S.; Fraser, B., Oversulfated chondroitin sulfate is a contaminant in heparin associated with adverse clinical events. *Nat. Biotechnol.* **2008,** *26* (6), 669.

70. Casu, B.; Guerrini, M.; Torri, G., Structural and conformational aspects of the anticoagulant and antithrombotic activity of heparin and dermatan sulfate. *Current pharmaceutical design* **2004,** *10* (9), 939-949.

71. Trowbridge, J. M.; Gallo, R. L., Dermatan sulfate: new functions from an old glycosaminoglycan. *Glycobiology* **2002,** *12* (9), 117R-125R.

72. Ronghua, H.; Yumin, D.; Jianhong, Y., Preparation and in vitro anticoagulant activities of alginate sulfate and its quaterized derivatives. *Carbohydr. Polym.* **2003,** *52* (1), 19-24.

73. Lin, C.-Z.; Guan, H.-S.; Li, H.-H.; Yu, G.-L.; Gu, C.-X.; Li, G.-Q., The influence of molecular mass of sulfated propylene glycol ester of low-molecular-weight alginate on anticoagulant activities. *European Polymer Journal* **2007,** *43* (7), 3009-3015.

74. De Zoysa, M.; Nikapitiya, C.; Jeon, Y.-J.; Jee, Y.; Lee, J., Anticoagulant activity of sulfated polysaccharide isolated from fermented brown seaweed Sargassum fulvellum. *Journal of Applied Phycology* **2008,** *20* (1), 67-74.

75. Mestechkina, N. M.; Shcherbukhin, V. D., Sulfated polysaccharides and their anticoagulant activity: A review. *Applied Biochemistry and Microbiology* **2010,** *46* (3), 267-273.

76. Alban, S.; Schauerte, A.; Franz, G., Anticoagulant sulfated polysaccharides: Part I. Synthesis and structure–activity relationships of new pullulan sulfates. *Carbohydr. Polym.* **2002,** *47* (3), 267-276.

77. Sun, X.-L.; Grande, D.; Baskaran, S.; Hanson, S. R.; Chaikof, E. L., Glycosaminoglycan mimetic biomaterials. 4. Synthesis of sulfated lactose-based glycopolymers that exhibit anticoagulant activity. *Biomacromolecules* **2002,** *3* (5), 1065-1070.

78. Zacharski, L. R.; Prandoni, P.; Monreal, M., Warfarin versus low-molecular-weight heparin therapy in cancer patients. *Oncologist* **2005,** *10* (1), 72-79.

79. Hanley, J. P., Warfarin reversal. *Journal of Clinical Pathology* **2004,** *57* (11), 1132-1139.

80. Pauli, R. M.; Madden, J. D.; Jeffery; Kranzler, K.; Culpepper, W.; Ronald, P., Warfarin therapy initiated during pregnancy and phenotypic chondrodysplasia punctata. *The Journal of Pediatrics 88* (3), 506-508.

81. Cotrufo, M.; De Feo, M.; De Santo, L. S.; Romano, G.; Della Corte, A.; Renzulli, A.; Gallo, C., Risk of warfarin during pregnancy with mechanical valve prostheses. *Obstetrics & Gynecology* **2002,** *99* (1), 35-40.

82. Healthwise. Partial Thromboplastin Time 2017. http://www.uofmhealth.org/health-library/hw203152 - hw203155.

83. Healthwise. Prothrombin Time and INR 2017. http://www.uofmhealth.org/health-library/hw203083 - hw203086.

84. A. V. Hoffbrand, P. A. H. M., Essential Haematology. 6 ed.; Wiley-Blackwell: 2011; pp. 315-329.

85. Turnbull, J. E., Getting the Farm Out of Pharma for Heparin Production. *Science* **2011,** *334* (6055), 462-463.

86. Updated Questions and Answers on Heparin Sodium Injection (Baxter). FDA: 2008.

87. Hedlund, K. D.; Coyne, D. P.; Sanford, D. M.; Huddelson, J., The heparin recall of 2008. *Perfusion-UK* **2013,** *28* (1), 61-65.

88. Powell, B. Heparin's Deadly Side Effects 2008. http://content.time.com/time/magazine/article/0,9171,1858870,00.html.

89. Conrad Hackett, D. M. Christians remain world's largest religious group, but they are declining in Europe 2017. http://www.pewresearch.org/fact-tank/2017/04/05/christians-remain-worlds-largest-religious-group-but-they-are-declining-in-europe/.

90. Panday, K.; Gona, A.; Humphrey, M. B., Medication-induced osteoporosis: screening and treatment strategies. *Therapeutic Advances in Musculoskeletal Disease* **2014,** *6* (5), 185-202.

91. Walenga, J. M.; Jeske, W. P.; Prechel, M. M.; Bacher, P.; Bakhos, M., Decreased prevalence of heparin-induced thrombocytopenia with low-molecular-weight heparin and related drugs. *Semin. Thromb. Hemost.* **2004,** *30*, 69-80.

92. Mazziotti, G.; Canalis, E.; Giustina, A., Drug-induced Osteoporosis: Mechanisms and Clinical Implications. *The American Journal of Medicine 123* (10), 877-884.

93. Rajgopal, R.; Bear, M.; Butcher, M. K.; Shaughnessy, S. G., The effects of heparin and low molecular weight heparins on bone. *Thromb. Res.* **2008,** *122* (3), 293-298.

94. Shaughnessy, S. G.; Hirsh, J.; Bhandari, M.; Muir, J. M.; Young, E.; Weitz, J. I., A histomorphometric evaluation of heparin-induced bone loss after discontinuation of heparin treatment in rats. *Blood* **1999,** *93* (4), 1231-1236.

95. Galambosi, P.; Hiilesmaa, V.; Ulander, V.-M.; Laitinen, L.; Tiitinen, A.; Kaaja, R., Prolonged low-molecular-weight heparin use during pregnancy and subsequent bone mineral density. *Thromb. Res.* **2016,** *143*, 122-126.

96. Toyoda, K., Antithrombotic Therapy for Pregnant Women. *Neurol. Med.-Chir.* **2013,** *53* (8), 526-530.

97. Douketis, J. D.; Ginsberg, J. S.; Burrows, R. F.; Duku, E. K.; Webber, C. E.; BrillEdwards, P., The effects of long-term heparin therapy during pregnancy on bone density - A prospective matched cohort study. *Thromb. Haemost.* **1996,** *75* (2), 254-257.

98. Barbour, L. A.; Kick, S. D.; Steiner, J. F.; Loverde, M. E.; Heddleston, L. N.; Lear, J. L.; Baron, A. E.; Barton, P. L., A prospective study of heparin-induced osteoporosis in pregnancy using bone densitometry. *Am. J. Obstet. Gynecol.* **1994,** *170* (3), 862-869.
99. Dahlman, T. C., Osteoporotic fractures and the recurrence of thromboembolism during pregnancy and the puerperium in 184 women undergoing thromboprophylaxis with heparin. *Am. J. Obstet. Gynecol.* **1993,** *168* (4), 1265-1270.
100. Khalil, H.; Davoudpour, Y.; Islam, M. N.; Mustapha, A.; Sudesh, K.; Dungani, R.; Jawaid, M., Production and modification of nanofibrillated cellulose using various mechanical processes: A review. *Carbohydr. Polym.* **2014,** *99*, 649-665.
101. Zimmermann, T.; Bordeanu, N.; Strub, E., Properties of nanofibrillated cellulose from different raw materials and its reinforcement potential. *Carbohydr. Polym.* **2010,** *79* (4), 1086-1093.
102. Wegner, T. H.; Jones, P. E., Advancing cellulose-based nanotechnology. *Cellulose* **2006,** *13* (2), 115-118.
103. Coughlan, M. P., CELLULOSE HYDROLYSIS - THE POTENTIAL, THE PROBLEMS AND RELEVANT RESEARCH AT GALWAY. *Biochem. Soc. Trans.* **1985,** *13* (2), 405-406.
104. Khalil, H.; Bhat, A. H.; Yusra, A. F. I., Green composites from sustainable cellulose nanofibrils: A review. *Carbohydr. Polym.* **2012,** *87* (2), 963-979.
105. Miao, C. W.; Hamad, W. Y., Cellulose reinforced polymer composites and nanocomposites: a critical review. *Cellulose* **2013,** *20* (5), 2221-2262.
106. Samir, M.; Alloin, F.; Dufresne, A., Review of recent research into cellulosic whiskers, their properties and their application in nanocomposite field. *Biomacromolecules* **2005,** *6* (2), 612-626.
107. Peng, B. L.; Dhar, N.; Liu, H. L.; Tam, K. C., Chemistry and applications of nanocrystalline cellulose and its derivatives: a nanotechnology perspective. *Can. J. Chem. Eng.* **2011,** *89* (5), 1191-1206.
108. Klemm, D.; Kramer, F.; Moritz, S.; Lindstrom, T.; Ankerfors, M.; Gray, D.; Dorris, A., Nanocelluloses: A New Family of Nature-Based Materials. *Angew. Chem.-Int. Edit.* **2011,** *50* (24), 5438-5466.

109. Teeri, T. T., Crystalline cellulose degradation: new insight into the function of cellobiohydrolases. *Trends in Biotechnology* **1997,** *15* (5), 160-167.

110. Kolakovic, R.; Peltonen, L.; Laukkanen, A.; Hellman, M.; Laaksonen, P.; Linder, M. B.; Hirvonen, J.; Laaksonen, T., Evaluation of drug interactions with nanofibrillar cellulose. *European Journal of Pharmaceutics and Biopharmaceutics* **2013,** *85* (3), 1238-1244.

111. Elazzouzi-Hafraoui, S.; Nishiyama, Y.; Putaux, J.-L.; Heux, L.; Dubreuil, F.; Rochas, C., The Shape and Size Distribution of Crystalline Nanoparticles Prepared by Acid Hydrolysis of Native Cellulose. *Biomacromolecules* **2008,** *9* (1), 57-65.

112. Beck-Candanedo, S.; Roman, M.; Gray, D. G., Effect of Reaction Conditions on the Properties and Behavior of Wood Cellulose Nanocrystal Suspensions. *Biomacromolecules* **2005,** *6* (2), 1048-1054.

113. Wang, Z.; Yao, Z.; Zhou, J.; Zhang, Y., Reuse of waste cotton cloth for the extraction of cellulose nanocrystals. *Carbohydr. Polym.* **2017,** *157*, 945-952.

114. Torlopov, M. A.; Mikhaylov, V. I.; Udoratina, E. V.; Aleshina, L. A.; Prusskii, A. I.; Tsvetkov, N. V.; Krivoshapkin, P. V., Cellulose nanocrystals with different length-to-diameter ratios extracted from various plants using novel system acetic acid/phosphotungstic acid/octanol-1. *Cellulose* **2018,** *25* (2), 1031-1046.

115. Araki, J.; Kuga, S., Effect of trace electrolyte on liquid crystal type of cellulose microcrystals. *Langmuir* **2001,** *17* (15), 4493-4496.

116. Bandyopadhyay-Ghosh, S.; Ghosh, S. B.; Sain, M., *The use of biobased nanofibres in composites*. Woodhead Publ Ltd: Cambridge, 2015; p 571-647.

117. Mihranyan, A., Cellulose from Cladophorales Green Algae: From Environmental Problem to High-Tech Composite Materials. *J. Appl. Polym. Sci.* **2011,** *119* (4), 2449-2460.

118. Kumar, A.; Negi, Y. S.; Choudhary, V.; Bhardwaj, N. K., Characterization of Cellulose Nanocrystals Produced by Acid-Hydrolysis from Sugarcane Bagasse as Agro-Waste. *Journal of Materials Physics and Chemistry* **2014,** *2* (1), 1-8.

119. Plackett, D. V.; Letchford, K.; Jackson, J. K.; Burt, H. M., A review of nanocellulose as a novel vehicle for drug delivery. *Nord. Pulp Paper Res. J.* **2014,** *29* (1), 105-118.

120. Abitbol, T.; Rivkin, A.; Cao, Y.; Nevo, Y.; Abraham, E.; Ben-Shalom, T.; Lapidot, S.; Shoseyov, O., Nanocellulose, a tiny fiber with huge applications. *Current Opinion in Biotechnology* **2016,** *39*, 76-88.

121. Camarero Espinosa, S.; Kuhnt, T.; Foster, E. J.; Weder, C., Isolation of Thermally Stable Cellulose Nanocrystals by Phosphoric Acid Hydrolysis. *Biomacromolecules* **2013,** *14* (4), 1223-1230.

122. Wang, B.; Sain, M., Isolation of nanofibers from soybean source and their reinforcing capability on synthetic polymers. *Compos. Sci. Technol.* **2007,** *67* (11-12), 2521-2527.

123. Dong, X. M.; Revol, J.-F.; Gray, D. G., Effect of microcrystallite preparation conditions on the formation of colloid crystals of cellulose. *Cellulose* **1998,** *5* (1), 19-32.

124. Hasani, M.; Cranston, E. D.; Westman, G.; Gray, D. G., Cationic surface functionalization of cellulose nanocrystals. *Soft Matter* **2008,** *4* (11), 2238-2244.

125. Lin, C. W.; Lin, J. C., Surface characterization and platelet compatibility evaluation of surface-sulfonated chitosan membrane. *J. Biomater. Sci.-Polym. Ed.* **2001,** *12* (5), 543-557.

126. Kusch, D., Sulfur Trioxide—Pyridine Complex, a Versatile Organic Reagent. *ChemInform* **2008,** *39* (2).

127. Gilbert, E. E., The Reactions of Sulfur Trioxide, and Its Adducts, with Organic Compounds. *Chem. Rev.* **1962,** *62* (6), 549-589.

128. Zoppe, J. O.; Peresin, M. S.; Habibi, Y.; Venditti, R. A.; Rojas, O. J., Reinforcing Poly(ε-caprolactone) Nanofibers with Cellulose Nanocrystals. *ACS Applied Materials & Interfaces* **2009,** *1* (9), 1996-2004.

129. Ramires, E. C.; Dufresne, A., A review of cellulose nanocrystals and nanocomposites. *Tappi J* **2011,** *10* (4), 9-16.

130. Ishihara, K.; Nomura, H.; Mihara, T.; Kurita, K.; Iwasaki, Y.; Nakabayashi, N., Why do phospholipid polymers reduce protein adsorption? *Journal of Biomedical Materials Research: An Official Journal of The Society for Biomaterials, The Japanese Society for Biomaterials, and the Australian Society for Biomaterials* **1998,** *39* (2), 323-330.

131. Kidoaki, S.; Matsuda, T., Adhesion forces of the blood plasma proteins on self-assembled monolayer surfaces of alkanethiolates with different functional groups measured by an atomic force microscope. *Langmuir* **1999,** *15* (22), 7639-7646.

132. Dee, K. C.; Puleo, D. A.; Bizios, R., *An introduction to tissue-biomaterial interactions*. John Wiley & Sons: 2003.

133. Shen, J. I.; Winkelmayer, W. C., Use and Safety of Unfractionated Heparin for Anticoagulation During Maintenance Hemodialysis. *American Journal of Kidney Diseases* **2012,** *60* (3), 473-486.

134. . Dialysis 2017. https://www.kidney.org/atoz/content/dialysisinfo.

135. Polaschegg, H. D., The Extracorporeal Circuit. *Semin. Dial.* **1995,** *8* (5), 299-304.

136. Safadi, S.; Albright, R. C.; Dillon, J. J.; Williams, A. W.; Alahdab, F.; Brown, J. K.; Severson, A. L.; Kremers, W. K.; Ryan, M. A.; Hogan, M. C., Prospective Study of Routine Heparin Avoidance Hemodialysis in a Tertiary Acute Care Inpatient Practice. *Kidney International Reports* **2017,** *2* (4), 695-704.

137. Cronin, R. E.; Reilly, R. F., Unfractionated Heparin for Hemodialysis: Still the Best Option. *Semin. Dial.* **2010,** *23* (5), 510-515.

138. Al Salloum, H.; Saunier, J.; Tfayli, A.; Yagoubi, N., Studying DEHP migration in plasticized PVC used for blood bags by coupling Raman confocal microscopy to UV spectroscopy. *Materials Science and Engineering: C* **2016,** *61*, 56-62.

139. Gayathri, N. S.; Dhanya, C. R.; Indu, A. R.; Kurup, P. A., Changes in some hormones by low doses of di (2-ethyl hexyl) phthalate (DEHP), a commonly used plasticizer in PVC blood storage bags & medical tubing. *Indian Journal of Medical Research* **2004,** *119* (4), 139.

140. Bis(2-ethylhexyl) Phthalate (DEHP) Summary Risk Assessment Report Joint Research Centre European Commission: Institute for Health and Consumer Protection, 2008.

141. Nichols, P. E.; Bates, J. S.; Sparks, T. D., Exploration of Polytetrafluoroethylene as a Potential Material Replacement for Hemodialysis Applications. *MRS Advances* **2016,** *1* (29), 2147-2153.

142. Nie, C.; Ma, L.; Xia, Y.; He, C.; Deng, J.; Wang, L.; Cheng, C.; Sun, S.; Zhao, C., Novel heparin-mimicking polymer brush grafted carbon nanotube/PES composite membranes for safe and efficient blood purification. *Journal of Membrane Science* **2015,** *475*, 455-468.

143. Tsai, H.-A.; Huang, D.-H.; Ruaan, R.-C.; Lai, J.-Y., Mechanical Properties of Asymmetric Polysulfone Membranes Containing Surfactant as Additives. *Industrial & Engineering Chemistry Research* **2001,** *40* (25), 5917-5922.

144. Li, S.-S.; Xie, Y.; Xiang, T.; Ma, L.; He, C.; Sun, S.-d.; Zhao, C.-S., Heparin-mimicking polyethersulfone membranes – hemocompatibility, cytocompatibility, antifouling and antibacterial properties. *Journal of Membrane Science* **2016,** *498*, 135-146.

145. Foster, E. J.; Moon, R. J.; Agarwal, U. P.; Bortner, M. J.; Bras, J.; Camarero-Espinosa, S.; Chan, K. J.; Clift, M. J. D.; Cranston, E. D.; Eichhorn, S. J.; Fox, D. M.; Hamad, W. Y.; Heux, L.; Jean, B.; Korey, M.; Nieh, W.; Ong, K. J.; Reid, M. S.; Renneckar, S.; Roberts, R.; Shatkin, J. A.; Simonsen, J.; Stinson-Bagby, K.; Wanasekara, N.; Youngblood, J., Current characterization methods for cellulose nanomaterials. *Chem. Soc. Rev.* **2018,** *47* (8), 2609-2679.

146. Ehmann, H. M. A.; Mohan, T.; Koshanskaya, M.; Scheicher, S.; Breitwieser, D.; Ribitsch, V.; Stana-Kleinschek, K.; Spirk, S., Design of anticoagulant surfaces based on cellulose nanocrystals. *Chem. Commun.* **2014,** *50* (86), 13070-13072.

147. Hoeng, F.; Denneulin, A.; Neuman, C.; Bras, J., Charge density modification of carboxylated cellulose nanocrystals for stable silver nanoparticles suspension preparation. *J. Nanopart. Res.* **2015,** *17* (6), 14.

148. Espinosa, S. C. 3D-Multilayered Cellulose Nanocrystal based Biocomposites for Articular Cartilage Tissue Engineering. University of Fribourg, 2014.

149. Chai, Q. Y.; Huang, Y. S.; Ayres, N., Shape Memory Biomaterials Prepared from Polyurethane/Ureas Containing Sulfated Glucose. *J. Polym. Sci. Pol. Chem.* **2015,** *53* (19), 2252-2257.

150. Soni, B.; Hassan, E. B.; Mahmoud, B., *Chemical isolation and characterization of different cellulose nanofibers from cotton stalks*. 2015; Vol. 134, p 581-589.

151. Karim, Z.; Hakalahti, M.; Tammelin, T.; P Mathew, A., *In situ TEMPO surface functionalization of nanocellulose membranes for enhanced adsorption of metal ions from aqueous medium*. 2017; Vol. 7, p 5232-5241.

152. Vongchan, P.; Sajomsang, W.; Subyen, D.; Kongtawelert, P., Anticoagulant activity of a sulfated chitosan. *Carbohydrate Research* **2002,** *337* (13), 1239-1242.

153. Sun, X. L.; Grande, D.; Baskaran, S.; Hanson, S. R.; Chaikof, E. L., Glycosaminoglycan mimetic biomaterials. 4. Synthesis of sulfated lactose-based glycopolymers that exhibit anticoagulant activity. *Biomacromolecules* **2002,** *3* (5), 1065-1070.

154. Grunkemeier, J. M.; Tsai, W. B.; Horbett, T. A., Co-adsorbed fibrinogen and von Willebrand factor augment platelet procoagulant activity and spreading. *Journal of Biomaterials Science, Polymer Edition* **2001,** *12* (1), 1-20.